Morphodynamics of Estuarine Channel Networks

MSc. Thesis
Arya Pamungkas Iwantoro
4299744

Earth Surface and Water
Track: Coastal Dynamics and Fluvial Systems
Faculty of Geosciences
Utrecht University

Morphodynamics of Estuarine Channel Networks

A.P. Iwantoro

Student Number: 4299744

Supervisors:

Dr. M. van der Vegt

Prof. Dr. M. G. Kleinhans

Version: Final version

Submitted: 9 March 2016

Earth Surface and Water

Track: Coastal Dynamics and Fluvial Systems

Faculty of Geosciences

Utrecht University

Abstract

The effects of tides on the morphodynamics of estuarine channel networks is still poorly understood. Whereas bifurcations in rivers are often morphologically unstable where one branch would be abandoned occurring avulsion. In more tide-dominated systems, these seem to be more stable in which the two downstream branches of bifurcation keep open. The main aim of this study was to understand the effects of tides on the morphological evolution of an idealized estuarine channel network. It consisted of an upstream river that bifurcates into two downstream channels that are connected to the sea. By analyzing the results obtained with a 2-Dimensional Hydrodynamics Delft3D model, we first identified the tidal propagation and sediment transport patterns in the system and subsequently examined the morphological development of the tidally-influenced junction. We analyzed four different scenarios. First, the branches of the junction were set up to be different in depth. Second, the branches of the junction were set to be different in length. In both scenarios, the tide at the mouth of both branches was equal. The effect of the tide on the stability of the junction was examined by varying the tidal amplitude. Third, the configuration of both branches was set to be equal, but the branches were forced with different tidal amplitude at the mouth. Fourth, a different tidal phase at the seaward of the branches is combined with the similar configuration of the branches. For the first and second scenario, the unequal geometry causes differences in tidal deformation along the channel, so the transport capacity in the branches becomes more unequal. As a result, the tides enhanced the morphological evolution that would occur in the absence of tides. For the third and fourth scenario, the different tidal forcing induces the tidal propagation from one branch to another. This propagation causes the erosion at the junction that maintains the two branches to keep open. These results indicate that equal tidal forcing enhances the morphological instability that would occur in a river only situation while the different tidal forcing can cause the junction to be more stable.

Contents

List of Figures

List of Tables

List of Symbols

a	reference height in the vertical direction in the water column	m
A_h	horizontal eddy viscosity	$m^2 s^{-1}$
AKSFAC	proportionality factor	-
AKSFAC*ks	Van Rijn's reference height factor	-
C	Chézy friction coefficient	$m^{1/2} s^{-1}$
c	sediment concentration	$kg\ m^{-3}$
c_{soil}	reference density of the sediment	$kg\ m^{-3}$
D_{50}	median grain size	m
e	Euler constant	-
$f(\theta)$	the magnitude of transverse slope effect	-
g	earth gravity acceleration	$m\ s^{-2}$
h	mean water depth	m
k	positive contant for nodal point relation by *Wang et al. (1995)*	-
K_h	horizontal eddy diffusivity	$m^2 s^{-1}$
ks	current-related effective roughness height	m
L_D	the length of downstream channels	km
L_u	the length of the upstream channel	km
L_w	e-folding length scale	m
M_2	semi-diurnal tidal component	-
M_4	quarter-diurnal tidal component	-
MorFac	Morphological acceleration factor	-
n	a degree of non-linearity of sediment transport to the depth-average flow velocity	-

Q_B	tidally-averaged bedload flux	$m^3\ s^{-1}$
Q_S	tidally-averaged suspended load flux	$m^3\ s^{-1}$
Q_W	river discharge	$m^3\ s^{-1}$
S	channel slope	m/m
SedThr	Minimum depth for sediment calculation	m
Thresh	Minimum sediment thickness for transport and erosion	m
u	depth-averaged velocity	$m\ s^{-1}$
U_0	tidal mean flow	$m\ s^{-1}$
U_{M2}	M2 velocity amplitude	$m\ s^{-1}$
V_0	tidal mean flow to the across channel direction	$m\ s^{-1}$
V_{M2}	M2 velocity amplitude to the across channel direction	$m\ s^{-1}$
W	the channel width	m
W_j	channel width at the Junction	m
x	a variable of distance in along channel direction	m
y	a variable of distance in across channel direction	m
z	a variable of distance in the vertical direction in the water column	m
$\langle\ \rangle$	bracket to denote the diurnal or semidiurnal tidally-averaged	-
Δt	the time step of calculation	s
Δx	along channel grid size	m
Δy	across channel grid size	m
η_{M2}	M2 water level/elevation amplitude	m
η_{M4}	M4 water level/elevation amplitude	m
λ_w	Adaptation length of flow	m
ρ_s	specific sediment density	$kg\ m^{-3}$
$\rho_{s,d}$	dry bed density	$kg\ m^{-3}$

ρ_w	the density of water	kg m^{-3}
ψ	asymmetry index: (var1-var2)/(var1+var2), where var1 and var2 is positive	-
τ_b	bed shear stress	Pa
τ_{cr}	critical bed shear stress	Pa
θ	non-dimensional shear stress (Shields parameter)	-
θ_{M2}	M_2 water level/elevation phase	rad
θ_{M4}	M_4 level/elevation phase	rad

1 Introduction

In river junctions, water and sediment are partitioned over the two downstream branches. Regarding sediment transport, the partitioning mechanism is necessary to river pattern evolution not only nearby the junction but also further away downstream. For instance, more sediment and weak flow in one branch might lead to the avulsion. Therefore, the dynamics of the junction are important to be understood to explain the past and to forecast the future evolution of the river.

In the absence of tidal forcing, river junctions are most likely to be morphologically unstable (*Kleinhans et al. 2008)*, where one bifurcate/branch would be abandoned. In the estuary, in which the tidal forcing is significant, the partitioning mechanism and morphodynamics of the channel networks are more complicated and poorly understood. Due to the tidal cycle, the current induced by tide changes in direction and magnitude periodically. During the peak flood, the river flow could be hampered by the tide whereas, during the ebb, the tidal flow is in the same direction as the river flow that increases the total flow to the seaward. The interaction could be different in each branch due to different friction, depth, length or other geometry differences of the branches. Those flow variations due to the tides affect the partitioning mechanism and, as a result, might be able to change the morphological stability of the bifurcation/junction.

Related to the civilization, the knowledge about the tidally-influenced junction becomes necessary since many deltas/estuaries in the world especially tide-dominated delta/estuary, have many channels connected to each other. Many of those are vital for civilization activities, such as for a transportation route to connect the civilization living on the upstream and the ocean (Nugrahadi, 2005). For instance, in Mahakam Delta and Fly Estuarine (Figure 1-1), the channel networks are also used as a shipping route for natural resources such as coal and woods from the upstream to the sea before they are distributed to other places. In the case of Mahakam Delta, the main transportation for the civilization is water transportation since people live in the delta which is surrounded by the channels. Thus, any changes in the channel networks give a significant impact to the life of the people as well as to the economic growth. For those reasons, the knowledge of tidally-influenced bifurcation/junction dynamics is very important to be understood for the delta and estuary spatial planning. Therefore, the main aim of my thesis is to improve our understanding of the morphodynamics of the junction forced by both river flow and tides.

Figure 1-1. An example of tidally-influenced junctions in Mahakam Delta (right), and Fly River Estuary (left) (Source: Google Earth™).

1.1 Previous Research on Morphodynamics of the River Junctions

To understand the morphological evolution of junctions, it is crucial to understand the division of water and sediment at the junction. Several previous studies have been done to analyze the mechanisms and factors involved in water and sediment partitioning in the river junction. The first theoretical analysis of the river junction stability was by *Wang et al. (1995)*. They proposed 'a nodal point relation' to determine the stability of the junction. The bed load transport (Q_B) in each branch depends on river discharge Q_w and the width of the branches (W). It is expressed by:

$$\frac{Q_{B1}}{Q_{B2}} = \left(\frac{Q_{w1}}{Q_{w2}}\right)^{k} \left(\frac{W_1}{W_2}\right)^{1-k} \tag{1-1}$$

Subscripted number (1 and 2) indicates the branches. k is a positive constant determined empirically. According to *Wang et al. (1995)*, the junction will be stable if k >n/3. Otherwise, one branch will be abandoned *(Kleinhans et al., 2013)*. n is an effective power of flow velocity to determine the bed load transport *(Kleinhans et al., 2008)*.

However, the bifurcation concept of *Wang et al. (1995)* have limitations. First, the value of k is unknown and varies in observations. Second, they assumed the water and sediment discharge are cross-sectionally uniform which is not in the case of asymmetrical transverse bed profile such as in meandering river bend.

Bolla Pittaluga et al. (2003) improved the 1-dimensional flow and sediment division analysis of *Wang et al. (1995)* to overcome the limitations of the earlier concept. *Bolla Pittaluga et al. (2003)* proposed that the junction behavior is mainly related to the hydraulic condition and local geometry of the upstream channel close to the junction (nodal point). The previous model was modified by allowing the transverse water and sediment transport due to the asymmetrical bed elevation in the cross section of the upstream channel just before the junction. This transversal effect can induce the asymmetric division of water and sediment to downstream channels and thereby influence the bifurcation stability. In the model of *Bolla Pittaluga et al. (2003)*, the equilibrium state of the junction depends on the Shields parameter in the upstream branches. The higher value of the Shields parameter gives the more stable equilibrium with the branches still open. In contrast, the lower value of the Shields parameter results in the junction instability where one channel will be abandoned, even with the small transverse bed elevation difference.

Kleinhans et al. (2008) conducted the junction stability analysis with the effect of a meandering bend in the upstream channels. The junction stability was tested for different radii and length of the upstream meandering bend, sediment grain size, and asymmetrical geometries of the downstream channels (length, width-depth ratio, and slope). The analysis was conducted on a 3D model, and the results were compared with the 1D nodal point relation model by *Pittaluga et al. (2003)* which has been modified by adding the meandering effect in the upstream channel.

According to *Kleinhans et al. (2008)*, the meandering bend in the upstream channel is essential for the division of sediment and river discharge since the channel curve causes a spiral flow just before the bifurcation in the transverse direction. Furthermore, the spiral flow causes transverse sediment transport that may induce different sediment concentration distribution on the left and right side of the upstream channel. The difference can lead to asymmetrical sediment transport division. Then the important factors for the river junction stability are:

- The gradient advantage of one of the downstream channels and length difference between branches cause unequal discharge in both branches. The discharge inequality leads to the instability of the junction caused by the distance to the sea with the influence of backwater adaptation length.
- A bend upstream can result in more flow in one channel and more sediment in the other. There will be more sediment to the downstream channel on the inner bend side while more water flow in the other side. The asymmetrical division of the water and sediment is due to the helical flow explained above.
- The width-depth ratio in the upstream channel determines the bar regime and evolution in the channel that is important to the dynamic of the junction.
- Sediment size and bed irregularity is also important to determine the morphological behavior of the bifurcation.
- The upstream meandering can be balanced by the slope advantage to get more stable junction.

Kleinhans et al. (2011) extended the *Pittaluga et al. (2003)* model by allowing width adjustments, based on the results of *Kleinhans et al. (2008).* The narrowing and widening of the downstream channel width due to bank erosion and deposition are considered since the width evolution strongly affects the junction development.

1.2 Previous Research on Morphodynamics of the Tidal Junctions

The tidal junction is a junction where the forcing is not only imposed by the river discharge upstream but also imposed by tidal forcing from the downstream. Theoretical studies on hydrodynamics of tidal junctions are limited. *Hill & Souza (2006)* used mass and momentum conservation to solve the frictionless tidal motion in a tidal channel networks with deep channels. The model successfully predicts the water level and phase in each channel. However, many tidal junctions have shallow depth where tidal nonlinearity is considerable. Based on Hill & Souza (2006), the river flow is ignored, while in many system it is a significant value which cannot be neglected. Therefore, the concept by *Hill & Souza (2006)* cannot be applied in morphodynamics modelling of the estuarine channel networks.

Buschman et al. (2010) explained the tidally-averaged flow division in tidal junction in the case of the downstream channels which have different length, depth, and roughness. To understand the impact of the tide in the flow division, the model used for each case was run into three forcing conditions: river only, tide only and tide and river forcing. Moreover, the flow division was determined by the average discharge in the downstream channels. The tidal discharge was obtained from the average tidal flow, which was determined by Stokes flux and the return flow, for two days during spring and neap tide. Then the discharge asymmetry index was used to analyze the asymmetrical degree of the average discharge division in the downstream channels.

$$\psi = \frac{\langle Q_w \rangle_1 - \langle Q_w \rangle_2}{\langle Q_w \rangle_1 + \langle Q_w \rangle_2} \qquad (1\text{-}2)$$

In which, $\langle Q_1 \rangle$and $\langle Q_2 \rangle$ are the average discharge in each downstream channel. The discharge asymmetry was observed in the spring and neap tide condition. According to *Buschman et al. (2010)*, it can be concluded that:

- Channel depth asymmetry condition

The presence of tidal motion enhances the asymmetric discharge distribution that would occur in a river-only situation. It is due to the fact that the roughness is less important in the deeper downstream branch. Therefore, the return discharge that compensates the Stokes flux in the deeper branch is larger than in the shallower one. It leads to the net discharge seaward in the deeper channel and the other way around in the shallower branch.

- Channel length influence

In river only case, shorter branch receives more discharge than a longer one. Then for river-tidal forcing case, the tidal forcing enhance the asymmetry. Tidal energy from the shorter channel partly propagates to the longer one that increases the tidal amplitude in the longer branch. This condition leads the higher water level in the longer branch and more river discharge is steered to the shorter branch.

- Bed roughness influence

In contrast to the other cases, the presence of tidal forcing in the junction gives the opposite effect to the river forcing related to the flow division. In the river-only condition, a smaller roughness branch conveys larger share of water discharge. On the other hand, tidal motion produces the net discharge from lower roughness channel to the higher one since in the channel with low roughness, the magnitude of Stokes flux is larger due to the small phase difference between flow velocity and water level. Therefore, in the constant river discharge, the dominant channel depends on the tidal range (spring-neap tide). In the spring tide situation, the dominant channel is the branch with higher roughness. However, in the neap tide condition the dominant channel is the branh with lower roughness.

Sassi et al. (2011) also used the same method as *Buschman et al. (2010)* to quantify the discharge asymmetry in the multiple bifurcations in Mahakam Delta. The discharge asymmetry inequality between river-only situation and combination forcing is quantified as a percentage of ψ-ψr/ ψr to determine the contribution of the tide to a change in the discharge division. The result shows that the increase of tidal effect seaward will increase the change of the discharge distribution.

Sassi et al. (2013) observed the secondary flow and suspended sediment distribution over a period of spring and neap tide from the field observation data. The paper implied that the secondary flow and transversal distribution of the suspended sediment in the junction channel are essential to water and sediment division. Further, the secondary flow and sediment distribution depend on the transverse bed profile of the upstream channel and the tidal motion.

1.3 Gaps in Knowledge

From *Kleinhans et al. (2008)*, it was known that, without tidal forcing, the different configuration of branches can lead to the unequal division of water and sediment where one channel receive larger share of water and/or sediment than the other. Then the asymmetric division causes one branch receives less sediment than its transport capacity and the bed erodes *(Wang et al., 1995; Pittaluga et al., 2003; Kleinhans et al., 2011)*. However, the hydrodynamics behavior and sediment division may change due to the tidal forcing from the seaward. Morphological instability of the river bifurcation might be enhanced by the tides. Otherwise, the tides might be able to counteract the morphological instability inducing morphologically stable bifurcation. It means that the tides could keep both branches open.

In the real life, the branches geometry could be different in length, width and depth. This situation will affect the tidal behavior and morphodynamics of the junction. The different geometry of branches might cause a different tidal deformation from the seaward to the upstream though the tide at the mouth of the branches is equal. The different tidal deformation might give an impact to the partitioning, either enhancing or counteracting the mechanism that occurs in the absence of tide.

Further, the different seaward tidal forcing can produce the different quantity of tidal forcing between branches. These tidal forcing asymmetries and phase differences between branches may also be able to change the division of water and sediment.

1.4 Objectives and Research Question

The aim of this study is to understand the role of tides in morphological evolution of the tidally-influenced junction. To address the objective, two primary cases are examined. The first case is junction geometry asymmetry combined by symmetrical tidal forcing between branches. In this case, the length or the depth of downstream channels is different, while at the seaward boundaries both branches are forced by the same tides. This case is conducted to get the insight if the equal tidal forcing between branches could counteract or enhance the morphodynamics that would occur in the river-only situation. The questions related to this case arise:

- *How does tide affect the sediment transport in tidally-influenced junction that has two branches with a different length or depth?*
- *What is the effect of the tides on the morphological evolution of the bifurcation channel that has two branches with a different length or depth?*

The second case is tidal forcing asymmetry between downstream channels. In this case, tidal amplitude or tidal phase imposed at the seaward boundary of the branches is unequal. In this case, the junction geometry is set up symmetrically. For this case, the questions are:

- *How does tide affect the sediment transport in tidally-influenced junction that has geometrically similar branches and is imposed by different tidal amplitude or phase between branches?*
- *What is the effect of the river-tide interaction in morphological evolution of the bifurcation channel that has two similar geometry branches and is imposed by different M2 elevation amplitude or phase in the two branches?*

1.5 Thesis Structure

Chapter 2 describes the approach used to answer the research questions and the method that has to be done for the chosen approach. Chapter 3 consists of the simulation results including their interpretation. Chapter 4 consists of a discussion about the outcome and the future study that could be conducted. In Chapter 5, the conclusion of this research thesis is provided. The complete overview of the result are given in the appendices.

2 Methodology

2.1 Research Approach

To reveal the role of the tides in morphological evolution of the tidal junction, idealized junction model should be built. There are two different approaches that can be undertaken to do so, which are using physical scaled and numerical model. Physical scaled model has more advantages for this study since it can imitate a real river situation on a smaller scale. However, it is costly and time-consuming since morphological evolution is a long-term process that could take in decades or even centuries. Besides, it takes more time to set up the channel in scaled model than setting up the model for numerical simulation.

Whereas numerical model is relatively simpler to be implemented and suitable for the long period of simulation. In this model, we can optimize and simplify the calculation as long as we can get the relevant feature of the process (in this study is morphological evolution). However, the quantity of the results that would be obtained depend on the sediment transport formulation that we use.

Since we are interested in the morphological behavior of the junction, the exact quantity of the sediment transport is not needed as long as the morphological evolution mechanism of the junction could be understood. Therefore, the idealized junction model is set up in the numerical modeling system. The modeling system used is Delft3D hydrodynamics model. It is the same model as used in *Kleinhans et al. (2008)* and *Buschman et al. (2010)*. The depth-averaged model (2DH) with 3D parameterization is used, which solves the unsteady shallow water equations. An overview can be seen in *Lesser et al. (2004)*. A two-dimensional model is selected instead of a one-dimensional model to allow the cross-channel flow and transport that may occur and become an important factor in flow and sediment division. Further, instead of a three-dimensional model, the two-dimensional model is preferred because the three-dimensional model is more computationally expensive and time-consuming to simulate a morphological evolution.

2.2 Model Setup

Parameter setting of the channel has to consider the bars regime development in the channel. According to *Kleinhans et al. (2008)*, the presence of the bars can change the water and sediment distribution at the junction. The bars development in the channel bank at some point would give feedback to hydrodynamics and sediment transport. Thus, letting the bar development in the absence of tide would complicate the analysis. Since it would be difficult to distinguish the effect of tide and the bars development in hydrodynamics and morphodynamics when the tides are involved. Therefore, the parameter setting should be set up to limit the bars development in the absence of tide.

First, to limit the bars development, it is necessary to set up the channel configuration by considering the bar regime that may occur in the channel. The bar regime is empirically predicted. The channel configurations and river discharge are the important factors to classify the bar regime. Several studies were conducted to classify the bar regime of the channel *(Parker, 1976; Struiksma et al., 1985; Mosselman, et al., 2006; Crosato & Mosselman, 2009; Kleinhans & van den Berg, 2010)*. According to those studies, the bar development can be prevented by setting up the channel configuration that only allow the bar regime in the overdamped condition as illustrated in Figure 2-1.

To determine the bar regime, *Struiksma et al. (1985)* identified characteristic length scales in the linearized equations for the steady alternate bars which are:

a. the adaptation length of flow λ_w (m):

$$\lambda_w = \frac{C^2 h}{2g} \tag{2-1}$$

where h is mean water depth and C is Chézy friction coefficient. g is gravity acceleration (9.81 m s^{-2} for earth).

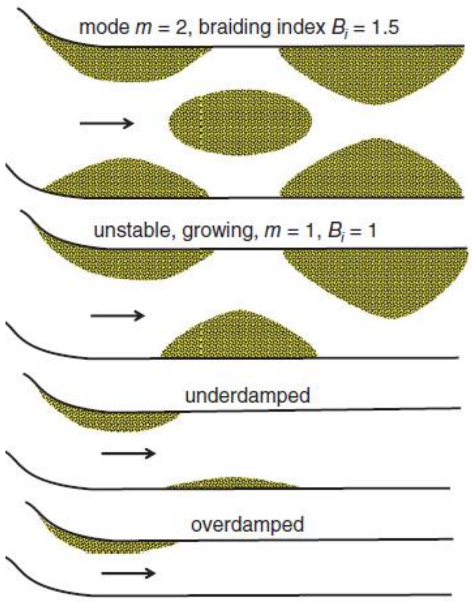

Figure 2-1. Definition of bar regime and mode ***(Kleinhans and van den Berg, 2010 after Parker, 1976; Struiksma et al., 1985; Mosselman et al., 2006; Crossato and Mosselman, 2009)*****.**

b. The adaptation length of a bed disturbance λ_s (m):

$$\lambda_s = \frac{h}{\pi^2}\left(\frac{W}{h}\right)^2 f(\theta)$$

(2-2)

where W is channel width and $f(\theta)$ is the magnitude of transverse slope effect calculated from an empirical function *(Koch & Flokstra, 1981; Talmon et al., 1995)*:

$$f(\theta) = 9\left(\frac{D_{50}}{h}\right)^{0.3}\sqrt{\theta}$$

(2-3)

where D_{50} (m) is the median sediment grain size and θ is non-dimensional shear stress (Shields parameter):

$$\theta = \frac{\tau_b}{(\rho_s - \rho_w) g D_{50}} \tag{2-4}$$

where ρ_s and ρ_w (kg m^{-3}) are water and sediment density. The shear stress (Pa) defined as:

$$\tau_b = \rho_w g R S \tag{2-5}$$

in which S (m^{-1}) is channel slope and R (m) is hydraulic radius defined as:

$$R = \frac{Wh}{W + h} \tag{2-6}$$

c. the wavelength of the bar L_p (m) calculated by:

$$\frac{2\pi\lambda_w}{L_p} = \sqrt{(n-1)\frac{\lambda_w}{\lambda_s} - \left(\frac{\lambda_w}{\lambda_s}\right)^2 - \left(\frac{n-3}{2}\right)^2} \tag{2-7}$$

where n is a degree of non-linearity of sediment transport to the depth-average flow velocity (q=*f*(u^n)).

d. Damping length of the bar L_D (m) calculated by:

$$\frac{\lambda_w}{L_D} = \frac{1}{2}\left(\frac{\lambda_w}{\lambda_s} - \frac{n-3}{2}\right) \tag{2-8}$$

The characteristic of the bars is a function of λ_s/λ_w, interaction parameter (IP). It depends significantly on the width-depth ratio (W/h) *(Kleinhans et al., 2008)*. For the narrow and deep channel, the bar is overdamped. Perturbation in the channel which may lead to the appearance of the bar results in only a small bar in the short distance downstream of perturbation or even no bar. For wider and shallower channel, the bars are underdamped. Disturbance in the channel can lead to over-deepening on the one side of the channel and enhancement of the bar on the other side across the channel. Then, if the channel is very shallow and wide, the bar will grow in height and number across the channel downstream of the perturbation.

Crosato & Mosselman (2009) proposed an empirical mode predictor from the theory of *Struiksma et al. (1985)* calculated by:

$$m^2 = \frac{0.17g(n-3)}{\sqrt{\frac{\rho_s - \rho}{\rho} D_{50}}} \frac{W^3 S}{C Q_W} \tag{2-9}$$

where Q_W (m^3s^{-1}) is river discharge, and m can be used to determine braiding index B_i of the river defined as:

$$B_i = \frac{m-1}{2} + 1 \tag{2-10}$$

in which B_i is total active channel across the river width. A river is categorized single thread for $B_i \leq 1.2$, moderately braided for $1.2 \leq B_i \leq 3$ and braided for $B_i > 3$.

Beside the bar regime, empirical river pattern prediction in the absence of tide has to be considered in setting up the channel configuration. Though the junction model bank is set up to be fixed, if the river pattern is empirically predicted to be, for instance, braided, the bar might grow and form a braided river. Potential specific stream power (ω_{pv}) (W m^{-2}) is defined to set up the desired river pattern type (e.g. braided, meandering and immobile). It is calculated by:

$$\omega_{pv} = \frac{\rho g Q S}{W} \tag{2-11}$$

and according to *van den Berg (1995)*, discriminant river pattern type analysis for stream power versus median grain size of the sediment is empirically defined as:

$$\omega_{bm} = 900 {D_{50}}^{0.42} \tag{2-12}$$

the parameter setting that has to be arranged to get stable river pattern and overdamped bar regime are median grain size (D_{50}) of the sediment, sediment density (ρ_s), water density (ρ_w), bed roughness, river discharge (Q_w), channel depth (h), slope (S) and width (W). The sediment type used for this study is sand, so D_{50} uses the median grain size of medium sand (0.25 mm) with the specific density (ρ_s) of 2650 kg m^{-3}, the reference density (c_{soil}) and dry density ($\rho_{s,d}$) of 1600 kgm^{-3} (typical sand density). There are two sediment sources in this study. First, the sediment concentration imposed from the upstream boundary. The imposed sediment from the upstream is set to be constant with the value of 0.1 kg m^{-3} during the simulation. The second sediment source is from the river bed. The properties of the sediment (grain size, settling velocity and sediment density) from the upstream and the bed are uniform. The sediment concentration is not imposed from the downstream boundary at the seaward of the branches

The water density is set to be uniform with the value of 1025 kg m^{-3}. The bed roughness uses the Chézy friction coefficient with the value of 60 $m^{1/2}s^{-1}$. The river discharge is set up to be constant with the value of 2800 $m^3 s^{-1}$. The channel depth is 15 m for the entire channel except for the case of downstream channels depth difference, and the channel slope is $3x10^{-5}$ m^{-1}. The channel width of the upstream channel just before the junction (W_j) is 480 m, and it converges 20 km upstream from the junction with the e-folding length scale for width (L_w) about 50 km calculated as:

$$y = W\ e^{-x/L_w} \tag{2-13}$$

After 20 km to the upstream, the upstream channel is straight with the length of 200 km to make sure the river dampen out smoothly *(Buschman et al., 2010)*. The width of the straight part of the channel is about 321 meter. Further, the upstream channel splits into two downstream channels with the same width. Both channels also diverge exponentially up to 30 km (except for the scenario with different branches length) to the downstream boundary with the same e-folding length scale for width (L_w). The bars and channel pattern characteristics of several locations with the different width are shown in Figure 2-2. In the top figure of Figure 2-2, it can be seen that only the downstream end channel configuration is classified as moderately braided. However, it can be neglected since the location is far away downstream from the junction. The other places are successfully set up as a stable channel with an overdamped bar regime in the absence of tidal motion.

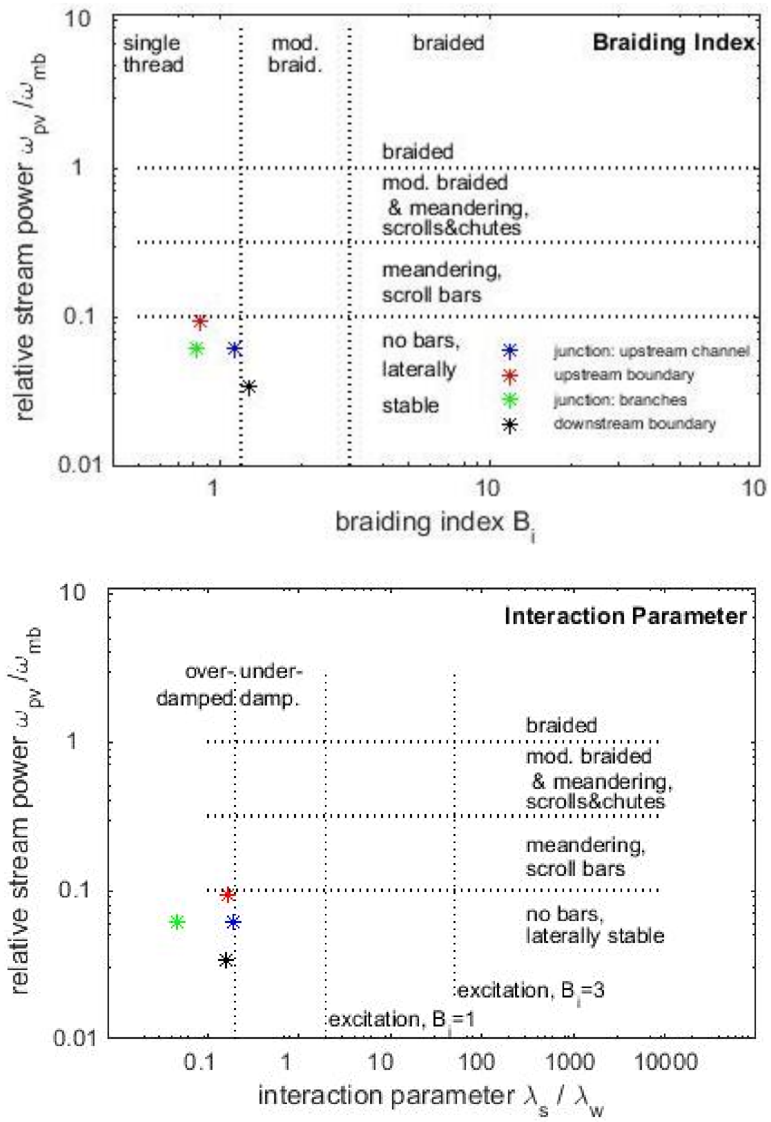

Figure 2-2. Bar regime and channel pattern classification at four locations of the channel with different width.

The other parameter used for flow and sediment transport calculations for the model is turbulence characteristics of the flow. Turbulence model used in this study is constant coefficient. A constant value leads to parabolic vertical velocity flow (laminar flow). The constant that must be input are horizontal eddy viscosity and diffusivity. Both values are set up to 1 $m^2 s^{-1}$ and 10 $m^2 s^{-1}$, respectively.

The Sediment transport calculation used is a formulation for non-cohesive sediment proposed by *van Rijn (2001)*. Sediment transport is distinguished into bedload and suspended load transport. In the model, those are classified by their vertical position in the water column *(van Rijn, 1993)*. Sediment transport below the reference height is classified as bedload, and that above the reference height is classified as suspended load. Reference height is defined as:

$$a = \min[\max(AKSFAC.ks; 0.01h), 0.2h] \tag{2-14}$$

in which AKSFAC is proportionality factor, ks is current-related effective roughness height. Multiplication of both variables is defined as 1 in this study.

Bedload transport is partly influenced by the bed level gradient. The bed level gradient or bed slope is distinguished into the slope to along channel direction and across channel direction. In along channel direction the bedslope effect is given by:

$$Q_B = \alpha_s Q_{B,x}' \tag{2-15}$$

while in transverse channel direction is expressed by:

$$Q_B = \alpha_s Q_{B,y}' \tag{2-16}$$

α_s is a term of bed slope effect. In along channel direction, the bed slope effect uses the predictor by *Bagnold (1966).* This predictor requires a self-defined parameter α_{bs} = 1 in this study. While the transverse slope effect uses *Ikeda (1982)* as presented by *Van Rijn (1993)* using a self-defined parameter α_{bn}= 1.5 in this study.

The grid used for the simulation is built in grid generation program developed by *Kleinhans et al. (2008)*. For the whole domain, the grid cell length to the along-channel direction (Δx) is fixed at 80 m. The grid cell length-width ratio is two at the junction and decreases gradually seaward since the grid cell width (Δy) increases due to the diverging channel width seaward and increases landward due to the converging channel upstream until 20 km upstream. The ratio is constant along the constant width part of the upstream channel. For the upstream channel, the channel width is divided equally by 12 grid cells across the channel. To split the channel, two grid cells are removed at the junction for the numerical reasons *(Kleinhans et al., 2008)*. Then each branch is set to gently curved on their side for the first 4 km from the junction. The branches width is divided equally into five grid cells across the channel. A time step of 6 seconds is used in all simulations to fulfill the requirement of Courant Number for numerical stability. The overview can be seen in *Stelling (1984)*. All the parameters setting used in the model are summarized and provided in Table 2-2.

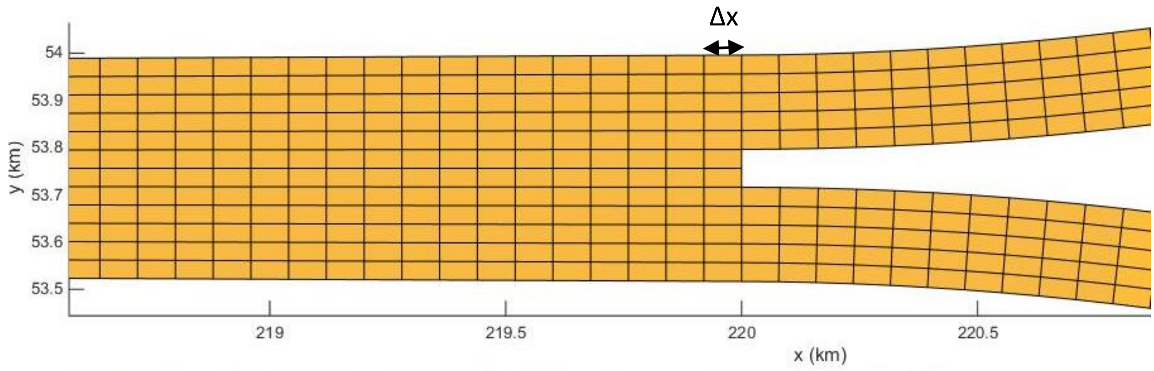

Figure 2-3. Grid set up of the junction

2.3 Scenarios

Several idealized junctions with different geometries and downstream tidal forcing are set up. First, the asymmetrical junction geometry is imposed with the same tidal amplitude and phase in the branches. This part is conducted to get the insight if tides could counteract or enhance the morphological evolution that would occur in a river only situation based on Kleinhans et. al. (2008). Second, the tidal amplitude and phase difference between branches are imposed in the symmetrical geometry junction. This setup is chosen to get the insight whether the different tidal forcing can cause morphological stability of the junction or force the junction to be unstable and occurring avulsion. Morphological stability in this term is when the two branches of the junction are maintained to keep open. While the morphological instability is when one branch tends to close off, occurring the avulsion.

Tidal forcing used in this idealized model are semi-diurnal (M_2) and quarter-diurnal (M_4) tides. The M_2 amplitude and phase are changed between different simulations while M_4 is set constant with the amplitude of 0.2 meters. Except in the river only case, the M_4 amplitude is set to 0. In the scenario with non-zero M_2 phase for each simulation, M_4 phase is configured to be twice as the M_2 phase at each seaward boundary.

Short-term and long-term simulation are undertaken for all scenarios. Long term simulation is conducted to find out the morphological evolution of the tidally-influenced junction in the long period. In this case, the morphological development in 100 years is examined. Since the long-term simulation is computationally expensive, the morphological acceleration factor (MORFAC) of the model has to be scaled up. The Morphological Acceleration Factor (MORFAC) alows the long-term morphodynamics evolution *(Lesser et al., 2004; Roelvink, 2006; Ranasinghe et al., 2011)* at time scales of decades *(Lesser, 2009; Tonnon et al., 2007, Jones et al., 2007, Lesser et al., 2004)* and centuries *(Dissanayake et al., 2009, Dissanayake et al., 2009, Van Der Wegen & Roelvink, 2008, van der Wegen et al., 2008)* to be done in the shorter simulation duration. The MORFAC value applied in this study is 200 with the simulation duration of 6 months.

Short-term simulation is done to explain the mechanism behind the morphological evolution from the long-term simulation. The hydrodynamics and sediment transport behavior in one M_2 period is observed to get the insight of the morphodynamics processes. The simulation is run for 10 days simulation duration to let the hydrodynamics being stable, and then the result from the last M_2 tidal cycle is examined. The bed update in the short-term simulation is inactivated to prevent the morphological feedback that might change the sediment transport and hydrodynamics process.

Four scenarios undertaken are described below.

1. Asymmetrical junction geometry and symmetrical tidal forcing between downstream channels

In the scenarios of this part, the tide imposed from the mouth of both branches has the same amplitude and phase. The first scenario is the case in which the depth of both branches is different and the second scenario is the case in which the length of both branches is different.

a. Depth difference between downstream channels

The depth of branch 2 (Figure 2-4) is set up as the initial parameter setting of the entire channel (15 meters) as determined according to bar theory explained in Section 2.2. The depth of branch 1 is set up to be shallower to get unstable condition where the shallower branch will close off (Kleinhans et al., 2008). Therefore, the depth of branch 1 is set up to be a half of the depth of branch 2 (7.5 meters). The depth change from the upstream channel to branch 1 is set up to change gradually from 15 meters to 7.5 meters for 2 km started from the junction up to seaward. It is conducted To avoid the reflection flow due to the rapid depth change.

In the short-term scenario, the tides imposed at the downstream of the branches is set to be equal. The simulations of this scenario are run six times with different M_2 elevation amplitude conditions which are without tide condition, 0.25 meter, 0.5 meters, 1 meter, 1.5 meters, and 2 meters.

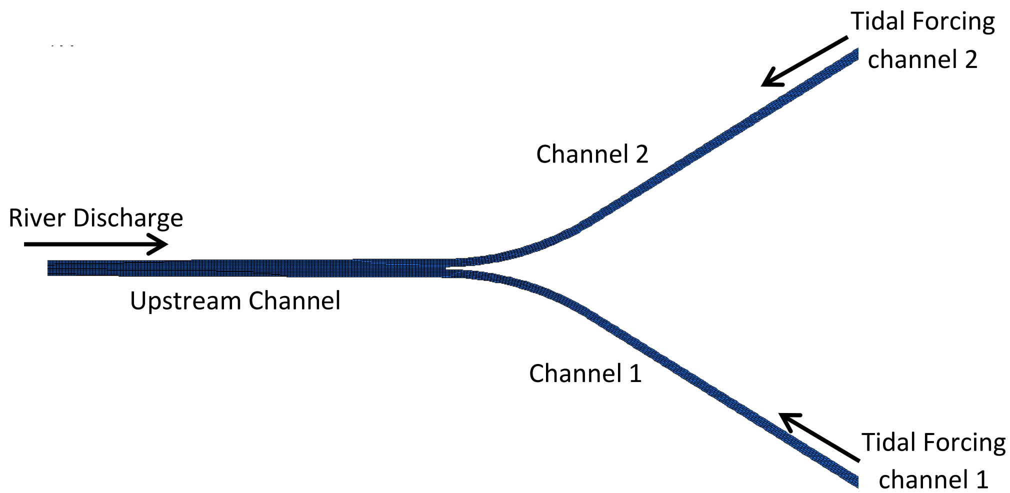

Figure 2-4. Junction illustration.

b. Length difference between downstream channels

The length of branch 2 is set up as an initial setting which is 30 km, and the length of branch 1 is set to be a half of the length of branch 2 (15 km). Then the tides imposed at the mouth of the branches are equal in amplitude and phase. The simulation repetition with different M_2 elevation amplitude is similar with the depth difference scenario.

2. Asymmetrical tidal forcing between downstream channels and symmetrical junction geometry

The scenarios in this part are for the junction that has symmetrical branches shape and geometry. On the other hand, the tidal forcing from downstream is set to be unequal between branches. The first scenario is that the M_2 elevation amplitude between branches is arranged to be different. While the second scenario is that the amplitude between branches is similar but, both phases are different. The M_4 amplitude and phase imposed from downstream are constant in the first scenario. In the second scenario, the M_4 amplitude at the downstream end of both branches is constant, but its phase is two times of the M2 phase at the branch with non-zero M_2 phase.

a. Tidal Elevation Amplitude difference between downstream channels

The junction geometry is arranged symmetrically, and different tidal amplitude is imposed from the downstream channels. The M_2 tidal elevation amplitude at the boundary of branch 2 is set up at 1 meter with the phase of 0. Then at the entrance of branch 1, M_2 tidal elevation amplitude is varied for each simulation which are without tidal condition, 0.25 meter, 0.5 meters, 1 meter, 1.5 meters, and 2 meters. The phase set up in all simulations is constant with the value of zero.

b. Tidal Elevation Phase difference between downstream channels

The junction geometry is arranged symmetrically, and different tidal phase is imposed on the downstream channels. The tidal amplitude forced from both the downstream channel boundaries is set up at 1 meter. Tidal phase at the boundary of branch 2 is set up at 0. Then at the entrance of branch 1, the M_2 tidal phase is varied for each simulation conducted in this scenario. The phase at the entry of branch 1 is varied with the value of 0, 22.5, 45, 67.5 and 90.

All the scenarios done is summarized in Table 2-1. While the parameter settings are provided in Table 2-2.

Table 2-1. Scenarios run and their geometry and tide setting.

Scenario	M_2 Amplitude (η_{M2}) (m)		M_2 Phase (θ) (deg)		Channel Length (L_D) (km)		Channel Depth (h) (m)	
	Branch 1	**Branch 2**	**Branch 1**	**Branch 2**	**Branch 1**	**Branch 2**	**Branch 1**	**Branch 2**
1.a. Length difference	0-2	0-2	0	0	15	30	15	15
1.b. Depth difference	0-2	0-2	0	0	30	30	7.5	15
2.a. M2 Amplitude difference	0-2	1	0	0	30	30	15	15
2.b. Tidal Phase difference	1	1	0-90	0	30	30	15	15

Table 2-2. Parameter Settings

Parameter	Symbol	Unit	Value
Channel and hydrodynamics Parameter Setting			
along channel grid size	Δx	m	80
channel slope	S	m^{-1}	$3x10^{-5}$
channel width at the Junction	W_j	m	480
Chézy friction coefficient	C	$m^{1/2}\,s^{-1}$	60
e-folding length scale	L_w	km	50
horizontal eddy diffusivity	K_h	$m^2\,s^{-1}$	10
horizontal eddy viscosity	A_h	$m^2\,s^{-1}$	1
length of the upstream channel	L_u	km	220
length of downstream channels	L_D	km	30
mean water depth	h	m	15
river discharge	Q_w	$m^3\,s^{-1}$	2800
time step of calculation	Δt	s	6
Sediment Parameter Setting			
dry bed density	$\rho_{s,d}$	kg m^{-3}	1600
imposed sediment concentration from the upstream	c	kg m^{-3}	0.1
median grain size	D_{50}	m	0.00025
reference sediment density	c_{soil}	kg m^{-3}	1600
specific sediment density	ρ_s	kg m^{-3}	2650
Morphology Parameter Setting			
along channel bed gradient factor for bedload transport	α_{bs}	-	1
minimum depth for sediment calculation	SedThr	m	0.1
minimum sediment thickness for transport and erosion	Thresh	m	0.05
morphological scale factor (long & short term, respectively)	MorFac	-	200 & 1
sediment layer thickness	-	m	25
transverse bed gradient factor for bed load transport	α_{bn}	-	1.5
Van Rijn's reference height factor	AKSFAC*ks	-	1

2.4 The Limitations of This Study

The junction model is highly idealized and simplified regarding geometry, but not on the physical processes. Thus, the result quantities depend on the setup and parameterization chosen. The limitations of the model are distinguished into two parts, the methods and related to the processes that would occur in the real situation.

Regarding the methods, two important factors affect the results. First is the selected grid size. In morphodynamics modeling, the results are sensitive to the grid resolution, mainly because the finer grid can represent the formation of local scour and bar development better than the coarser one *(Kleinhans et al., 2008)*. However, the computational cost must be taken into account, so the optimum size must be used to balance the result accuracy and the computational cost. Second, the sediment transport process depends on the sediment transport predictor including the bed slope effect term. The predictor is important to determine the sediment transport results as well as the morphological development since it can enhance or slow down the morphological processes.

In the real situation, the processes are indeed more complex. Several important processes that are neglected in the model would give a significant effect on the morphological development of bifurcation which are bank erosion, sediment sorting, and density difference. Firstly, related to the bank erosion, the widening or narrowing channel width due to the erosion strongly affect the bifurcation development *(Kleinhans et al., 2011)*. The channel width adaptation enables the branches to keep open while the fixed model shows the avulsion *(Kleinhans et al., 2011)*. The converging channel in the tide-dominated estuary is formed by the tide and also give the feedback to the tidal spatial deformation along the estuary. However, since the bank erosion is not involved in this model the converging channel only give the influence in tidal deformation without obtaining feedback. Second, in this study the bed and delivered sediment properties are uniform. In the estuaries, several sediment variety in the systems likely presents. This poorly sorted sediment might give a significant influence on the morphological development. The presence of gravel or rocks that has low erodibility can decrease the sediment entrainment and transport from and to the junction. As a result, it will also influence the morphological evolution of the junction. Furthermore, in this study, the sediment is only imposed from the upstream boundary and from the erosion of the river bed. The sediment is not imposed from the seaward boundaries.

In this study, the water density is set to be constant. In the real life, the estuarine is the place that fresh water from the river meets the saline water from the sea. Density difference and the related salt intrusion brought by the tides from the sea can induce substantial alterations of the water level gradients, and baroclinic pressure gradients need to be involved *(Buschman et al., 2010)*. Thus, the density difference *(de Swart, 2015)* might affect the sediment transport processes at the junction.

3 Result and Analysis

3.1 Symmetrical tidal forcing and asymmetrical junction geometry between downstream channels

3.1.1 Depth Difference Scenario

Figure 3-1 shows the erosion and deposition pattern for the river-only and river-tide case in several kilometers nearby the junction for a hundred years simulation. In both cases, the erosion occurs in the deeper branches. The erosion starts at the junction and expands downstream. Further, a bar develops in the upstream channel on the shallower branch side. Tides enhance the morphological evolution of the junction that occur in the river only case. The erosion in the deeper branch is larger and widens more rapidly than in the river only case. Furthermore, the bar in the upstream channel on the shallower branch side is more developed in height and length. However, the morphological development slows down after 20 years. It can be seen in Figure 3-2, in the river-tide case, the bar development in upstream channel grows very fast in the first 20 years. Though it still grows afterward, the growth rate is smaller than the first 20 years. While in the river only case, the bar development at the same location slowly develops in the first 70 years and grows more rapidly afterward. The bar seems to rise continually over a hundred years.

A fixed bar in the middle of the upstream channel just before the junction develops to the shallower branch side of the upstream channel (Figure 3-1). This bar development is enhanced by the presence of migrating bar that develops at the upstream channel where the channel start diverging and migrates downstream. This migrating bar causes a small silting up in the deeper branch that can be noticed in the year 50 of the tide-river case in Figure 3-1. However, after that, the deeper branch is eroded again. Whereas the migrating bar amplifies the fix bar development at the junction to be more developed to the shallower branch side of the upstream channel. Then the fixed bar expands more to the downstream in the shallower branch resulting in the silting up in the shallower branch.

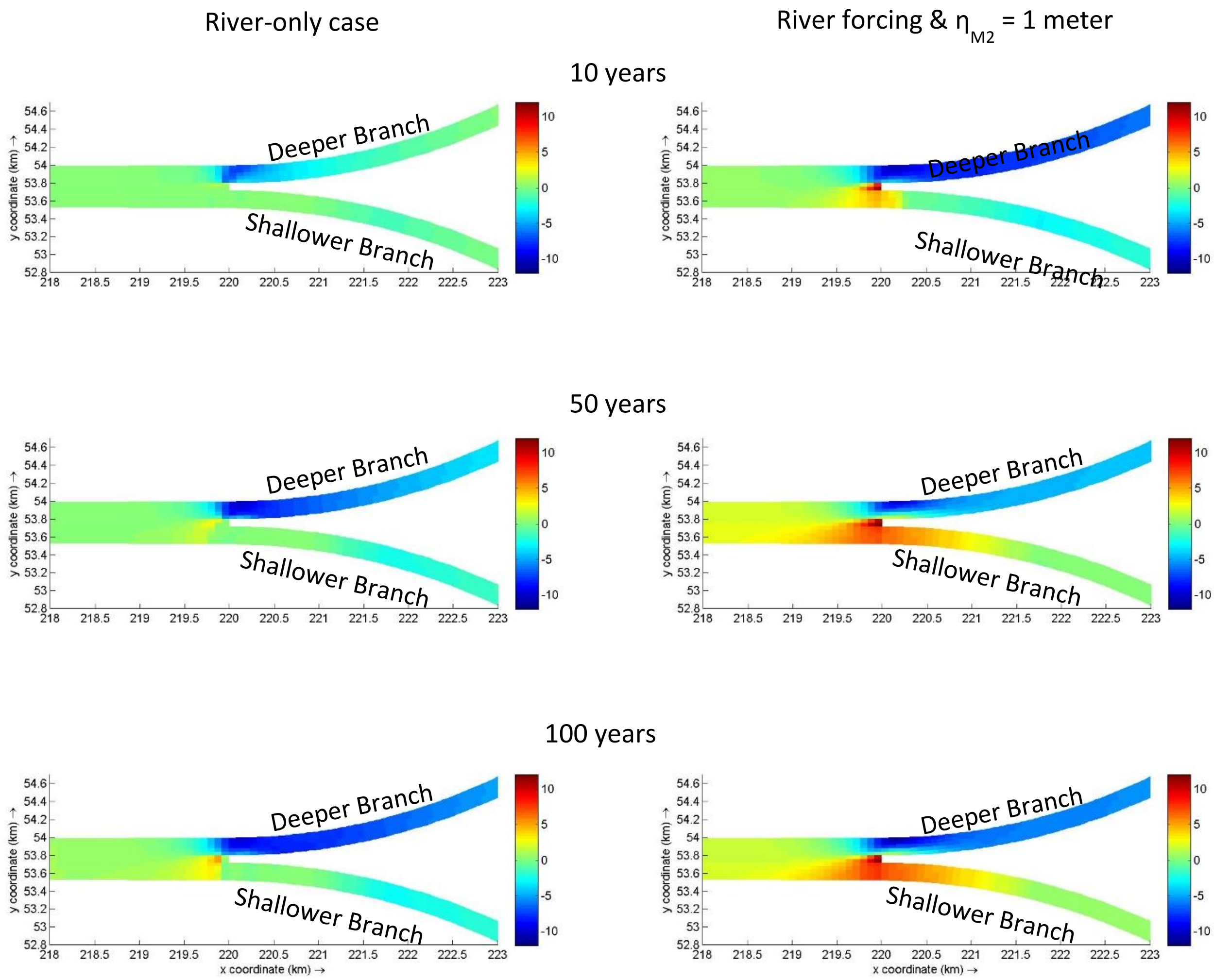

Figure 3-1. Erosion and deposition pattern of the junction for 100 years simulation several kilometers nearby the junction. The left panels are the case without tides, and the right panels are the case with the tides (M2 elevation amplitude = 1 meter).

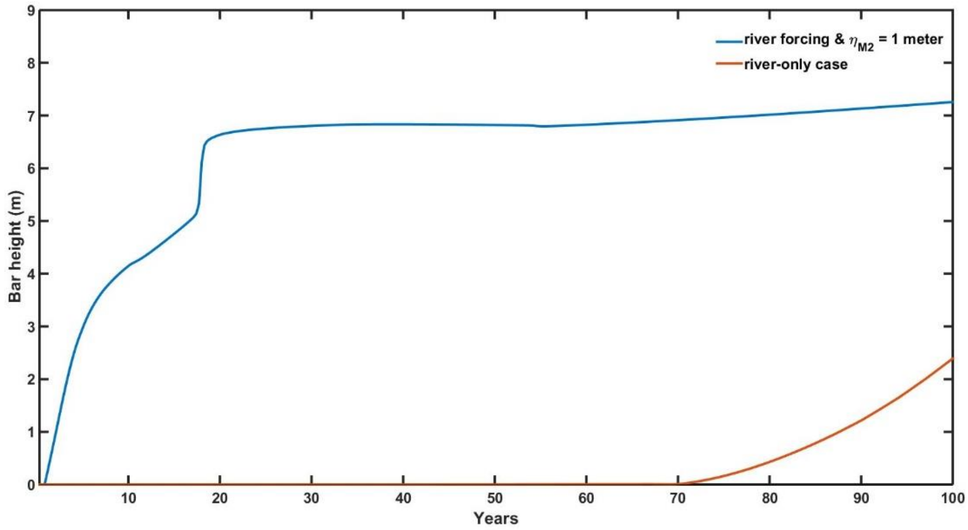

Figure 3-2. The bar height evolution at the shallower branch just after the junction for the river-tidal case and river only case.

A larger flow causes the erosion in the deeper branch. The larger flow in the deeper branch can be seen from the width-averaged and tidally-averaged mean flow (U_0) presented in Figure 3-3. Then the width-averaged M2 velocity amplitude (U_{M2}) in Figure 3-4. In Figure 3-3, it can be seen that the mean flow in the deeper branch is larger than in the shallower branch. The significant increasing mean flow changes nearby the junction in the shallower branch is due to the gradual depth change (from about 15 meters to 7.5 meters). The presence of the tide does not give a significant change for the mean flow in both branches. The flow direction is directed to the sea in all tidal conditions in the entire channel due to the large river discharge.

Figure 3-4 shows the spatial evolution of width-averaged M2 velocity amplitude (U_{M2}) for different tidal forcing. In the deeper branch, the U_{M2} is larger than in the shallower branch in the almost all location except around 5 kilometers from the sea boundary (between around km 45 and 50). The U_{M2} magnitude in the deeper branch increases from the sea to the junction. The opposite behavior of the U_{M2} spatial profile appears in the shallower branch. The U_{M2} decreases upstream and significantly decreases with the gradual deepening at the junction due to the gradual deepening. The spatial evolution of the U_{M2} in both branches is more apparent for a higher tidal forcing (Figure 3-4).

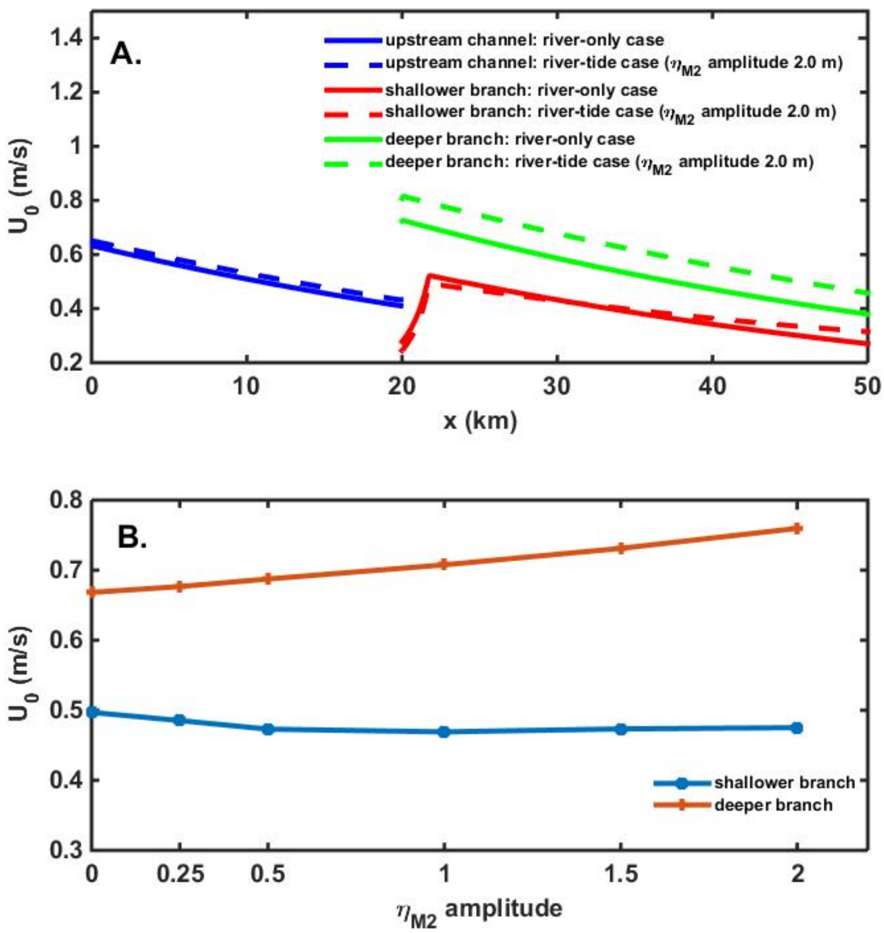

Figure 3-3. A) The width-averaged mean flow (U_0) profile along the channel for depth-difference branches in the absence of tide (solid line) and with the M2 tidal water level amplitude of 2 meters (dash line). Km 0 at the most left of the graph is the most upstream of the upstream channel at which the channel start diverging seaward. B) The mean flow at 4 km from the junction in both branches for different M2 elevation amplitude imposed from the sea. The positive mean flow indicates the flow is to the seaward direction.

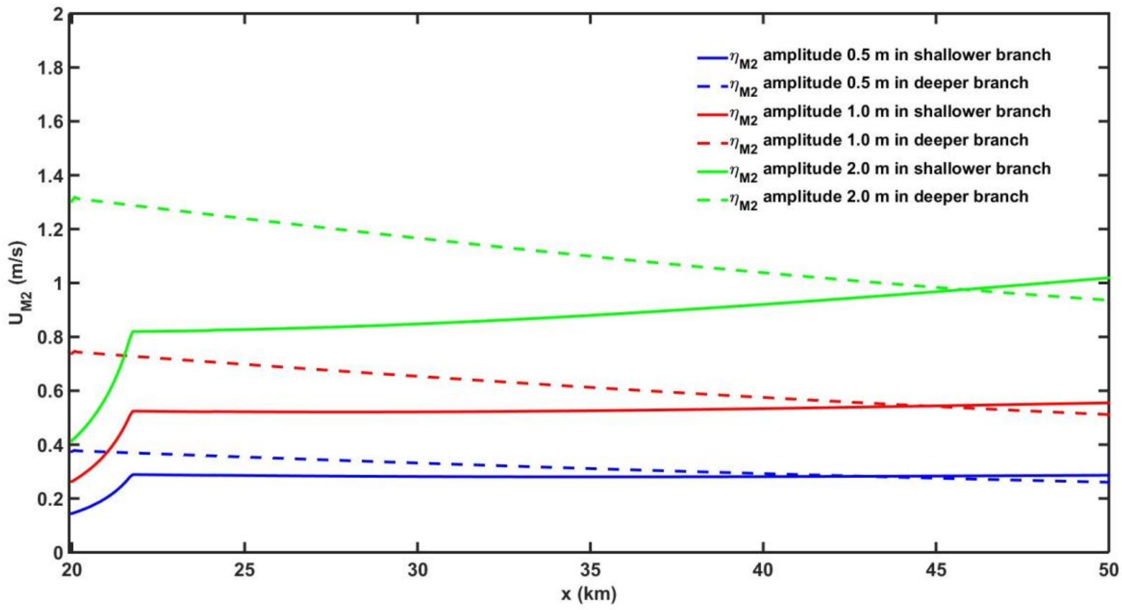

Figure 3-4. The width-averaged M2 velocity amplitude (U_{M2}) spatial profile along the shallower branch and the deeper branch. Km 20 indicates the junction while km 50 is the sea boundary of the branches.

The U_{M2} seems to control the sediment transport quantity. In other word, it determines the quantity of the sediment entrained from the bed. While the mean flow controls the sediment transport dominant direction. Figure 3-5 shows tidally-averaged suspended load flux (Q_S) in both branches with different tidal forcing condition. Regarding direction, Q_S is directed to the sea for the entire channel caused by the mean flow to the sea direction. Regarding the quantity, Q_S becomes larger for the larger tidal forcing indicating that the U_{M2} steers the sediment entrainment. In the deeper branch, Q_S shows the increasing behavior upstream indicating that erosion takes place at this location confirmed by the long-term simulation. In the shallower branch, Q_S gradually decreases from the sea boundary to the junction. It is much dropped in the location of gradual channel deepening nearby the junction. The very low Q_S at the junction in the shallower branch side is caused by the weak mean flow and U_{M2} at this location. As a result, the deposition presents at this location causing the bar development as shown in the long-term simulation. The similar behavior of sediment flux is also shown for bedload sediment flux which can be seen in Figure 3-6.

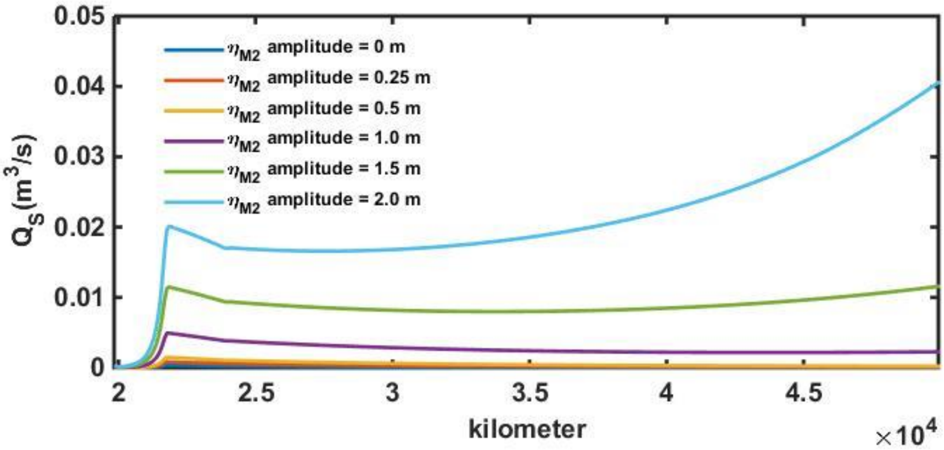

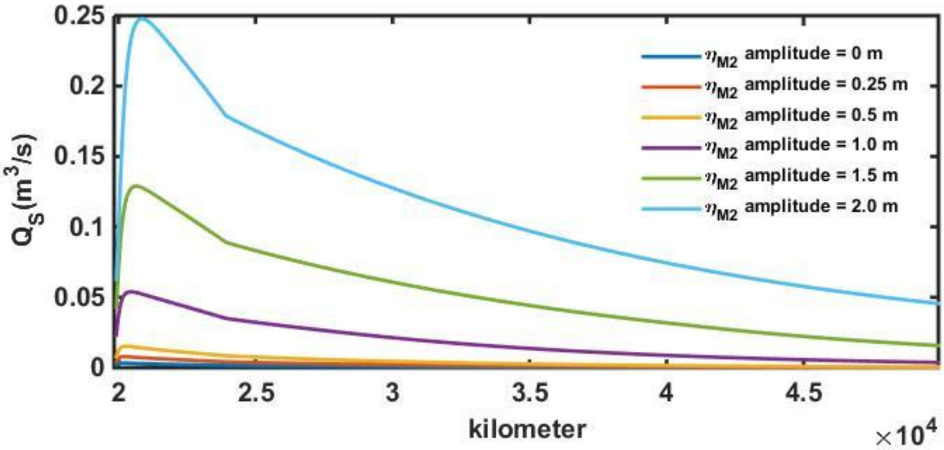

Figure 3-5. Tidally-averaged suspended load flux (Q_S) profile along the shallower branch (channel 1) (top figure) and the deeper branch (channel 2) (bottom figure) for different tidal amplitude imposed from the seaward of both branches.

The M2 tides cross current amplitude (V_{M2}) and tidally-averaged cross flow (V_0) in the upstream channel just before the junction are shown in Figure 3-7. The positive value of mean cross flow (V_0) indicates that the flow is more dominant to the deeper branch. The cross-flow magnitude does not seem to be sufficient to erode the bar development in the middle of the upstream channel. Furthermore, main direction to the deeper branch indicates that, more water is conveyed to the deeper branch. More water into this branch induces the larger flow into this branch causing the erosion while the shallower branch experiences the opposite process. Less water discharged into the shallower branch causes the sediment brought from the upstream to settle at the junction on the shallower branch side. As a result, the silting up occur, and the bar develops at this location. The silting up in one branch and erosion in the other increases the inequality of the flow and as a feedback enhances the morphological process in the branches.

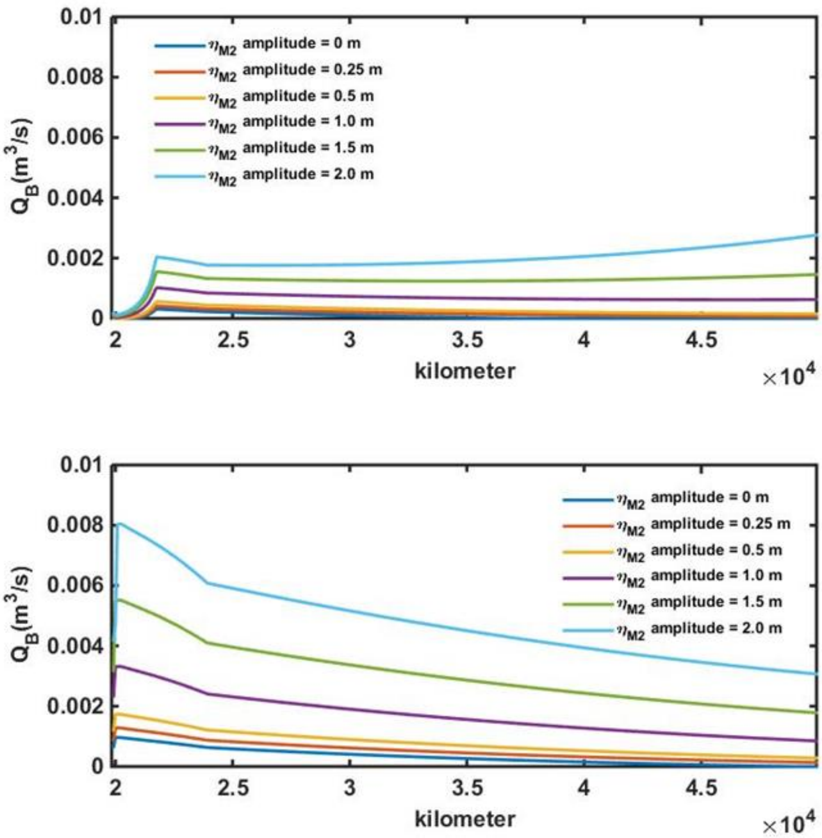

Figure 3-6. Tidally-averaged bedload sediment flux (Q_B) profile along the shallower branch (top panel) and the deeper branch (bottom panel) for different tidal amplitude imposed from the seaward of both branches.

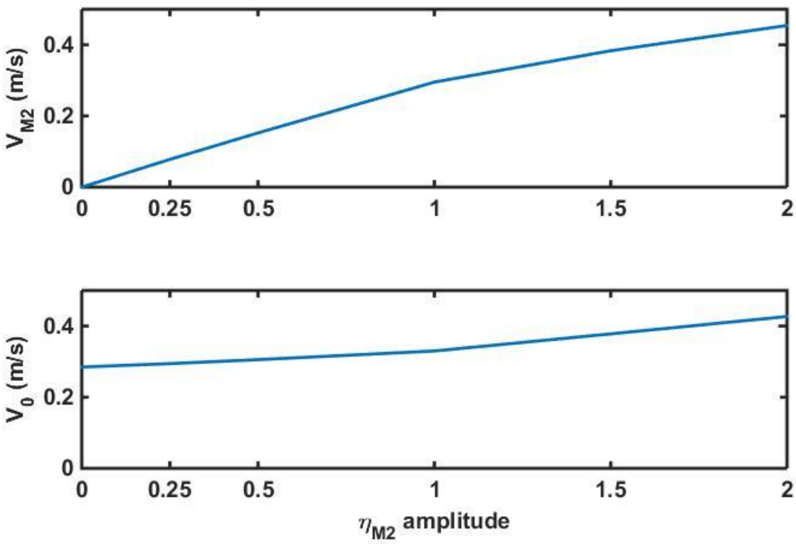

Figure 3-7. The M_2 tidal flow (top panel) and the mean flow (bottom panel) to the cross-channel direction in the middle of the upstream channel just before the channel bifurcates for the different tidal situations.

Even though from the short-term simulation, we know that tides enhance the sediment transport, it cannot fully predict the long-term morphological evolution. From Figure 3-1, it can be seen that the erosion location in the deeper branch expands downstream. While the increasing of Q_S to the downstream that indicates erosion only appears in the first several kilometer after the junction and it is followed by the decreasing. In other words, the advection term of tidally-average sediment transport is less important to the morphological evolution. The bar development and non-linearity of sediment transport seem to be more important than the advection term. The non-linearity of sediment transport cause the larger erosion at the location that would erode in river-only situation and also amplification of the bar development. With the presence of tide, the large U_0 and U_{M2} in the deeper branch erodes the bars and continue deepening the branch. While the weak flow in the shallower branch leads the fix and migrating bar to be more developed to the shallower branch. Then the silting up gives the feedback to the flow and the non-linearity response of the sediment transport to the flow velocity enhances the branch silting up.

3.1.2 Length Difference Scenario

Figure 3-8 shows the differences in morphological evolution between the river only and the river-tide case. Similar to the depth difference scenario, the tides seem to enhance the morphological evolution that would occur in the river only situation. In the absence of tide, the shorter branch (the bottom branch in each panel) is eroded nearby the junction and the erosion expands downstream. On the other hand, the slight erosion occurs in a longer branch only in the first 40 years of the simulation and the scour starts to be filled with the sediment and that location then has a constant deposition trend.

In the presence of tide, the morphological evolution seems to be enhanced. In the first ten years, the sediment accumulation pattern, in this case, is almost similar to the river only situation in a hundred years. After ten years, the morphological evolution of the junction becomes more unequal. The deposition is enhanced by the migrating bar that comes from the upstream channel in which the channel start diverging. The deposition occurs in the longer branch causing a constant silting up in a hundred years which can be seen in Figure 3-9. Whereas erosion is shown in the shorter branch. The erosion seems to expand downstream occurring a channel deepening for the entire shorter branch. This condition could induce the channel avulsion where longer branch could be abandoned due to the siltation.

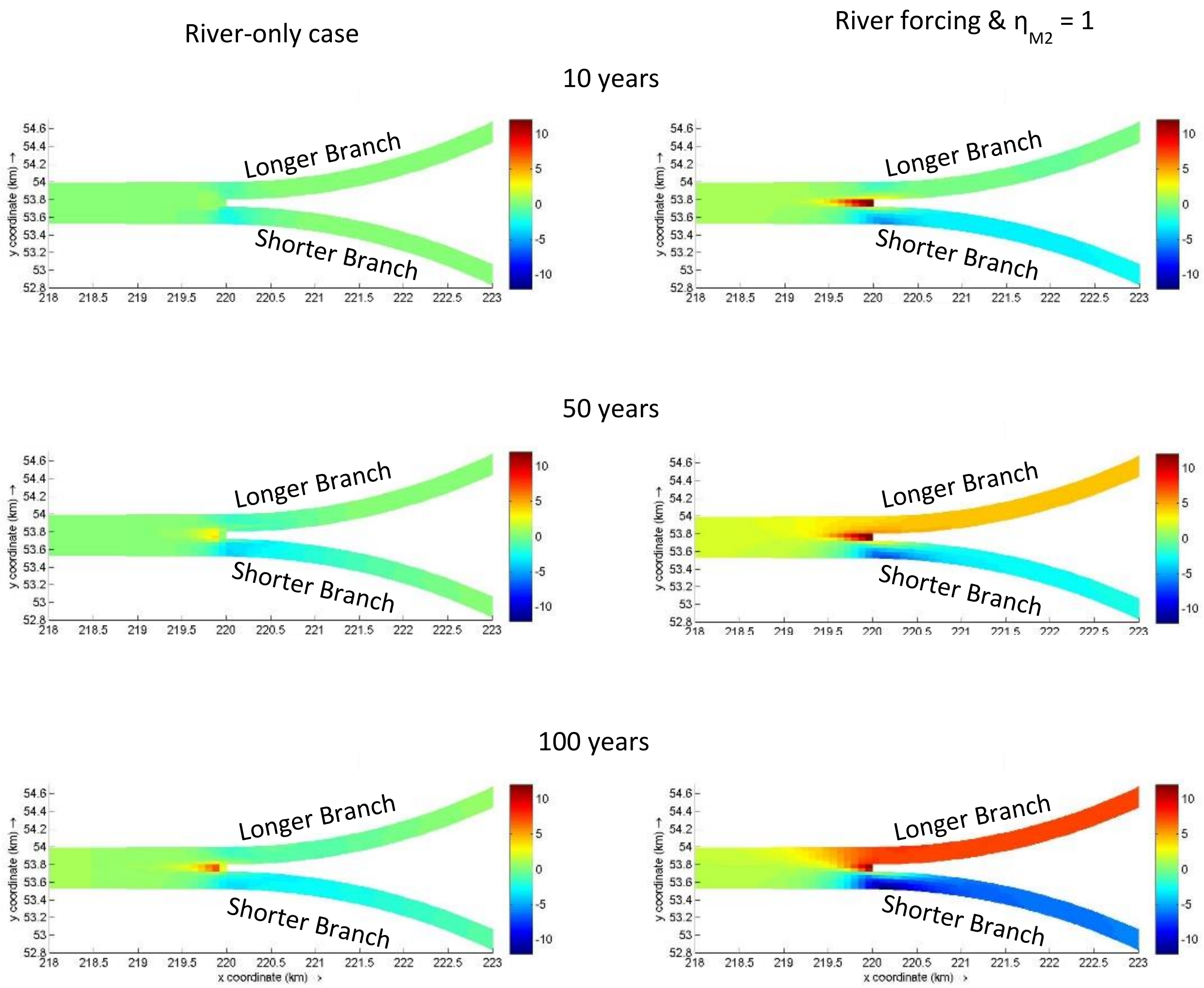

Figure 3-8. Erosion and deposition pattern for 100 years simulation several kilometers nearby the junction. The left panels are the case without tides, and the right panels are the case with the tides (M2 elevation amplitude = 1 meter).

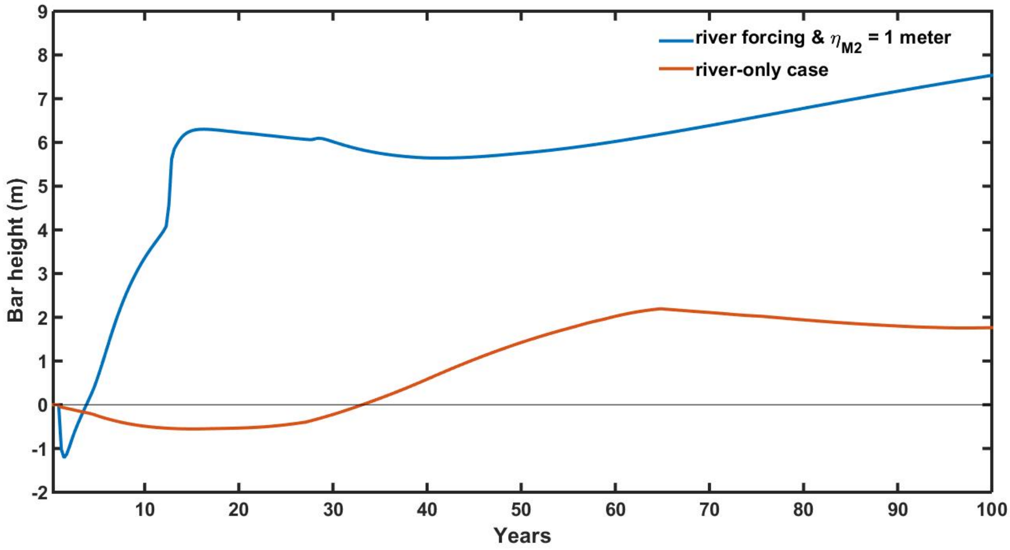

Figure 3-9. The erosion/deposition time series on the longer branch side of the upstream channel just before the channel bifurcates.

The unequal flow causes the morphological instability of the junction conveyed in both branches in which the shorter branch has larger flow than the longer one. The mean flow (U_0) and the along channel M_2 current amplitude (U_{M2}) spatial profile can be seen in Figure 3-10 and Figure 3-11. The flow inequality between branches is larger with the presence of the tide. The presence of migrating branch from the upstream amplifies the bed inequality in both branches. The weak flow in the lower branch and the non-linearity of sediment transport cause a silting up. In the absence of tide, the river flow magnitude in the shorter branch is higher than the longer one resulting in a larger transport capacity in the shorter branch. The presence of tides increases the inequality of the transport capacity since the U_{M2} in the shorter branch is also larger than in the longer branch. The more considerable U_{M2} in the shorter branch is caused by the shorter distance from the sea to the junction. In the shorter branch, tides reach the junction earlier and start feeding the upstream channel and longer branch with water. As a result, tides convey more water in the shorter branch. While in the longer branch, the tides are hampered by the tides coming from the shorter branch. Therefore, the U_{M2} in the longer branch is smaller. The large U_{M2} and mean flow in the shorter branch induces a larger transport capacity in that branch, so the migrating bar is eroded in this branch. Whereas a small transport capacity due to a weak flow in the longer branch is insufficient to transport the sediment from the upstream and erodes the migrating bar. It can be said that The tides cause the system to be more dynamics. Thus, more sediment is transported from the upstream due to the local bed erosion upstream, and the migrating bar also comes faster to the junction and is larger than in the river only situation. The insufficient transport capacity in the longer branch causes the sediment to be deposited and, therefore, the branch silt up and has a high possibility to close off.

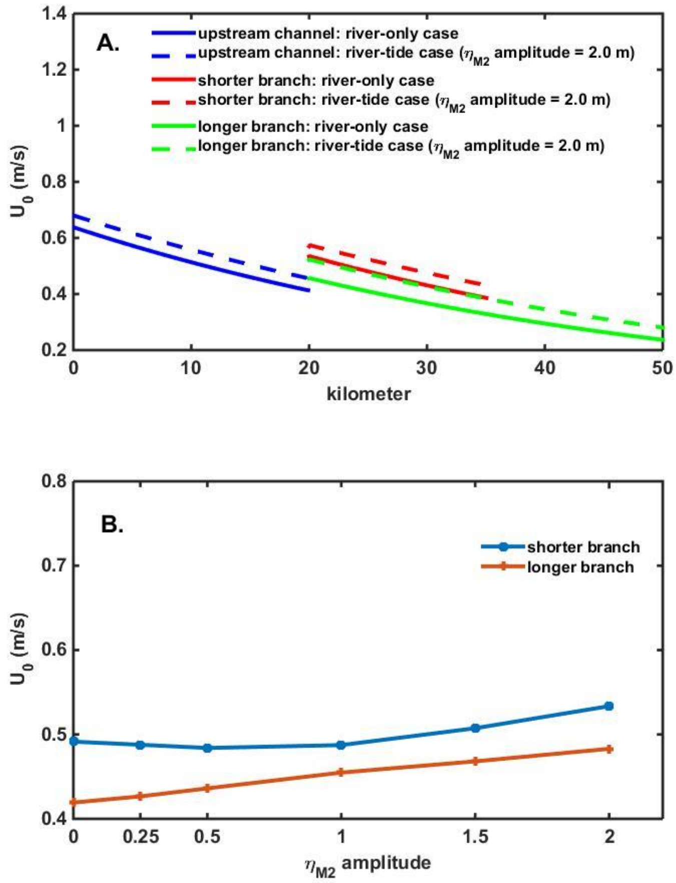

Figure 3-10. A) The width-averaged mean flow (U_0) profile along the channel for the river-only case and river-tide case (M_2 water level amplitude of 2 meters). Km 0 at the most left of the graph is the most upstream of the upstream channel at which the channel start diverging seaward. B) The mean flow at 4 km from the junction in both branches for different M2 elevation amplitude imposed from the sea.

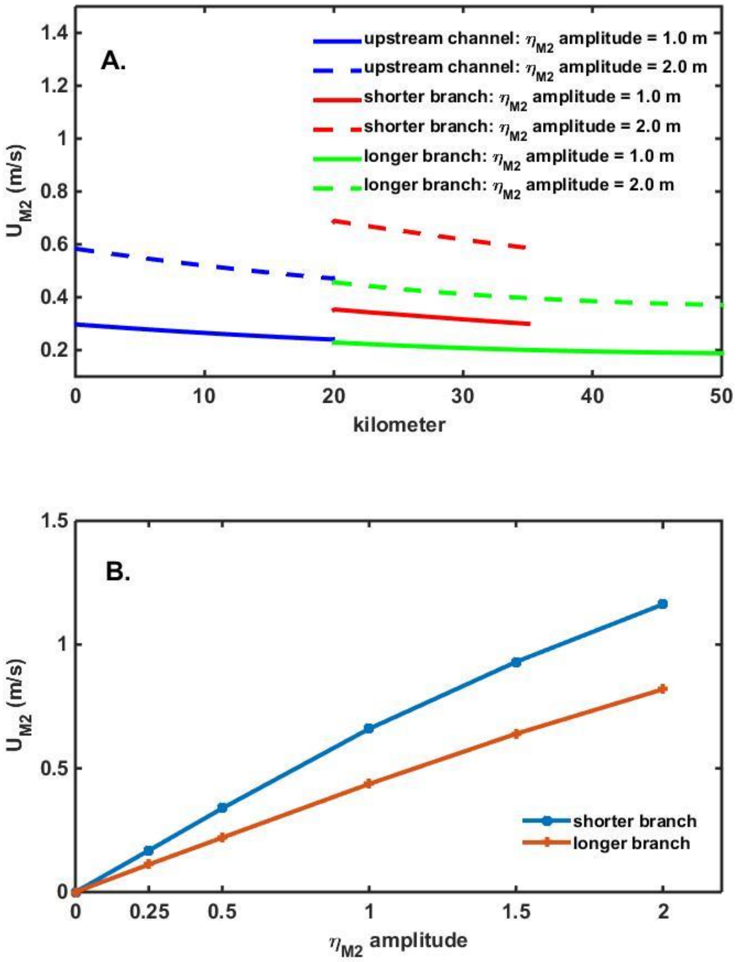

Figure 3-11. A) The width-averaged M2 velocity amplitude (U_{M2}) profile along the channel for length-difference branches for the case of M_2 water level amplitude of 1 meter and 2 meters. Km 0 at the most left of the graph is the most upstream of the upstream channel at which the channel start diverging seaward. B) The mean flow at 4 km from the junction in both branches for different M2 elevation amplitude imposed from the sea.

The different branch length also causes the different tidal celerity between branches. The celerity difference increases the cross flow at the junction that might erode the bar at the middle of the upstream channel. However, the cross-channel flow induces by propagation from channel 1 to channel 2 is weak and less significant for eroding the bar. Figure 3-12 shows the cross flow in the middle of the upstream branch just before the junction. From a bottom panel in Figure 3-12, it can be seen the tidally-averaged cross flow is to the shorter branch direction (negative indicates it is to shorter branch and positive is to the shorter branch). The mean cross flow magnitude is still below 0.1 m/s with the V_{M2} of 0.2 m/s for the largest tides case.

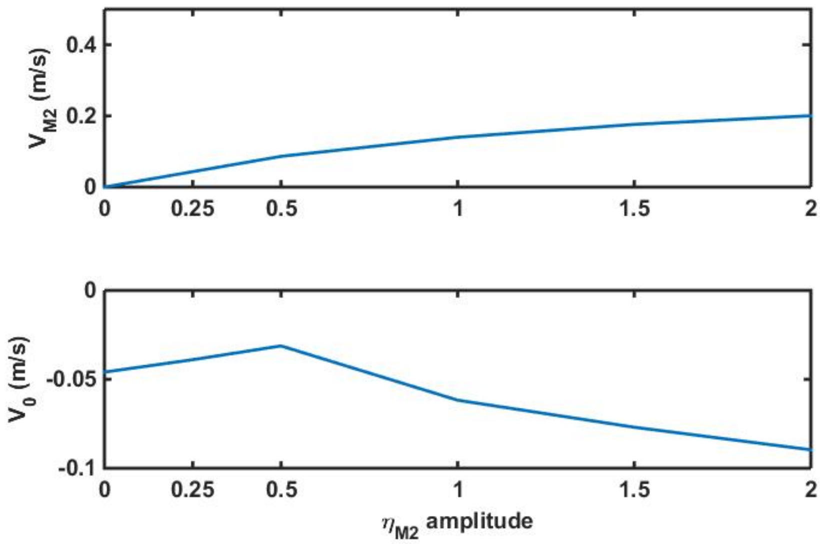

Figure 3-12. The M_2 tidal flow (top panel) and the mean flow (bottom panel) to the cross-channel direction in the middle of the upstream channel just before the channel bifurcates for the different tidal situations.

The morphological development of the junction is mainly caused by the bar development that is much enhanced with the presence of tides. The advection term in sediment transport is less important in determining the morphological development. It can be seen in the spatial pattern of tidally-averaged suspended load flux in Figure 3-13 and bedload flux in Figure 3-14. If the advection term is important, there will be erosion at the junction in both branches since the sediment flux is much increased from the junction toward downstream nearby the junction. However, the low flow and the presence of migrating bar silt up the longer branch. The non-linearity of the sediment transport seems to be more important. The non-linearity of the sediment transport enhances the silting up at this branch while the erosion is enhanced in the shorter branch.

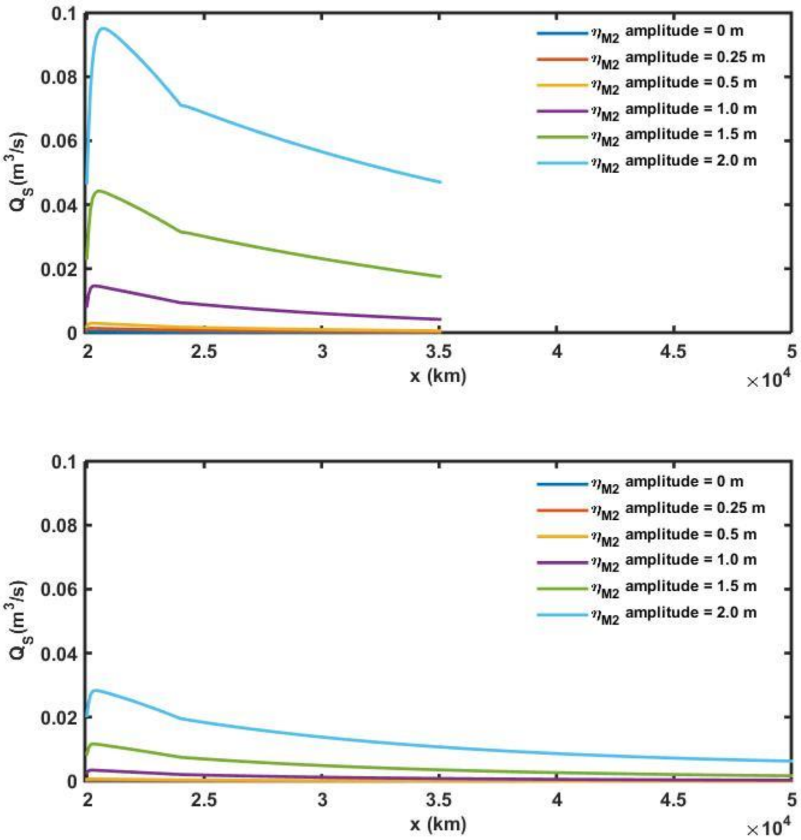

Figure 3-13. Tidally-averaged suspended load flux (Q_S) profile along the shorter branch (top panel) and the longer branch (bottom panel) for different tidal amplitude situation.

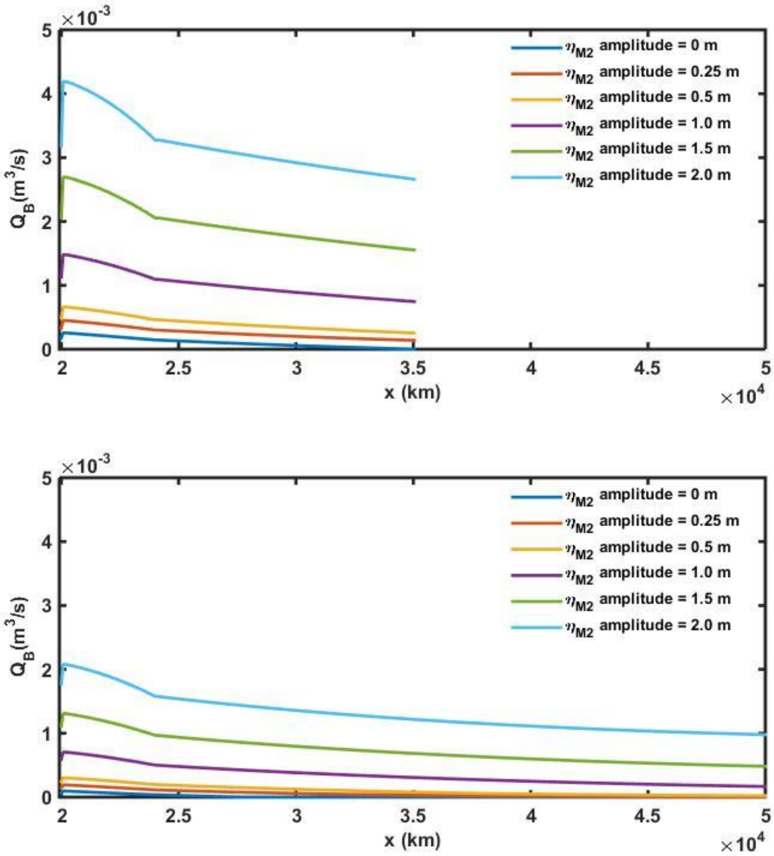

Figure 3-14. Tidally-averaged bedload flux (Q_B) profile along the shorter branch (top panel) and the longer branch (bottom panel) for different tidal amplitude situation.

3.2 Asymmetrical tidal forcing between downstream channels and symmetrical junction geometry

3.2.1 Tidal Elevation Amplitude Difference Scenario

Figure 3-15 shows the difference between the morphological development of the junction imposed by equal and different tidal amplitude in both branches. The unequal tidal forcing between branches results in the erosion at the junction. In both branches, the erosion occurs and expands downstream while the subtidal trench that connects the branches occurs in the upstream channel just before the junction. The unequal tidal forcing situation seems to erode a bar that occurs in equal tidal forcing case. The tides from the branch with larger tidal forcing propagates to the other branch to balance the weaker forcing and lower water level from the other branch.

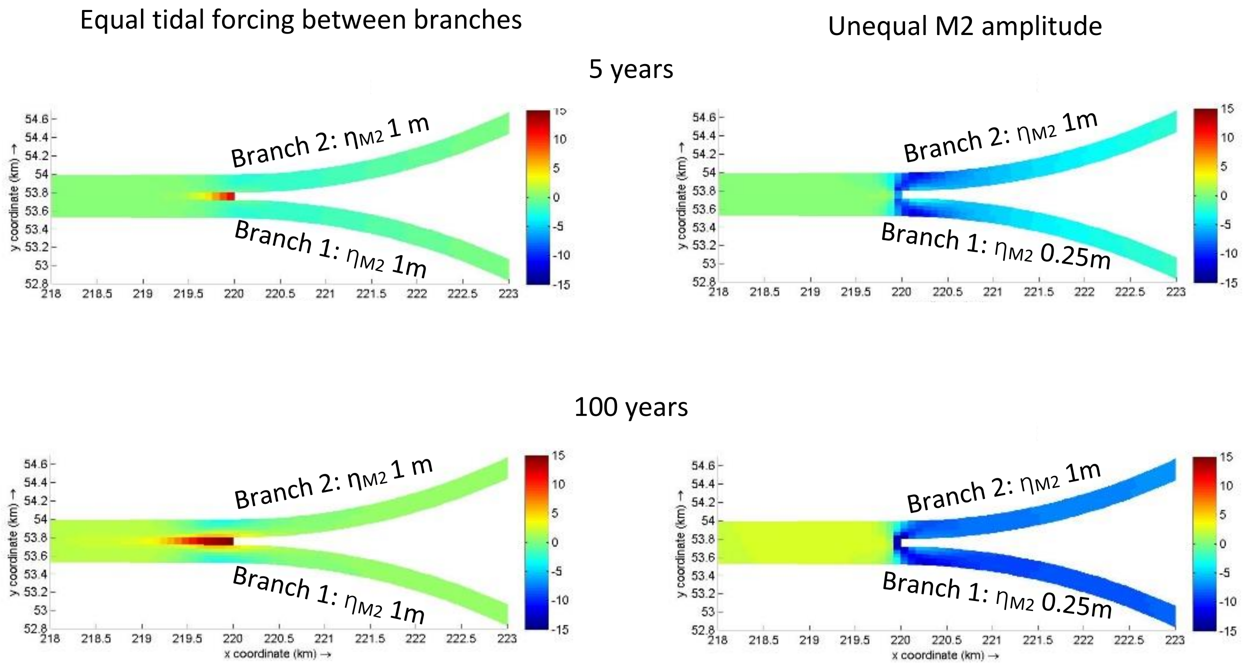

Figure 3-15. Erosion and deposition pattern for 100 years simulation at the junction. The left panels are the case with equal tidal forcing imposed between branches (M2 elevation amplitude of 1 meter). The right panels are the case with unequal tidal forcing between branches (M2 elevation amplitude in the lower branch (branch 1) = 0.25 meters; in the upper branch (branch 2) = 1 meter).

Figure 3-16 shows the cross flow in the middle of the upstream channel just before the junction for different tidal forcing in the branch 1 (lower branch in Figure 3-15). The tidally-averaged cross flow in the middle of the upstream channel just before the junction (bottom panel in Figure 3-16) is small with the magnitude lower than 0.1 m/s for all tidal condition. Though the mean cross flow is low, the M_2 tidal current in across channel direction V_{M2} is very large. It is larger when the tidal forcing difference between branches is increased. The small mean flow and large M_2 cross current indicate that the tidal current shift its direction over an M_2 period with almost the same magnitude. The large M_2 tidal current with this alternating direction causes the erosion at the junction in the upstream channel. Then it cancels the bar development that occurs in equal tidal forcing situation.

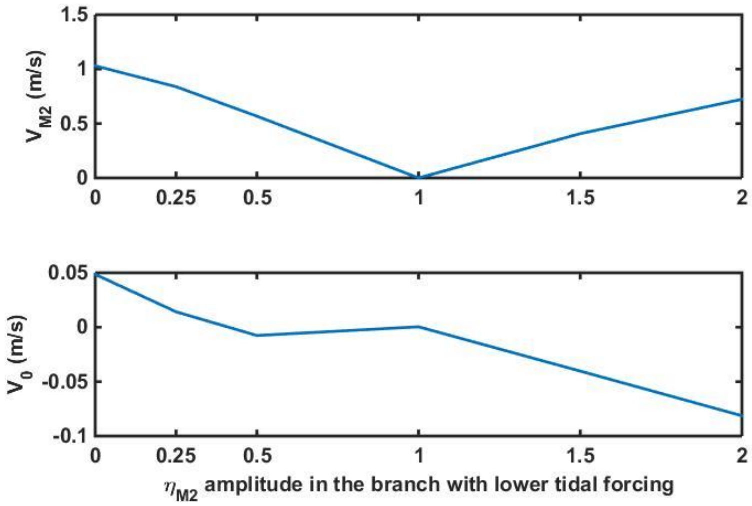

Figure 3-16. The M_2 tidal flow (top panel) and the mean flow (bottom panel) to the cross-channel direction in the middle of the upstream channel just before the channel bifurcates for the different tidal situations in the branch with varied tidal forcing (branch 1). While the branch 2 is imposed by the M_2 tide with the elevation amplitude of 1 meter.

The tidal amplitude inequality between branches also causes the opposite behavior of the mean flow and the M_2 tidal current in along channel direction (U_0 and U_{M2}) in both branches. A branch with larger tides has more considerable U_{M2} than in the other branch (Figure 3-17). While the mean flow is larger in the branch with weaker tides (Figure 3-18). This situation occurs because the river flow is discharged to the branch with weaker tidal forcing. Since larger river discharge and the tides from the other branch flow to this the branch with weaker tides, the U_{M2} in this branch is much hampered. Therefore, the U_{M2} becomes smaller. In the branch with larger tidal forcing, tides have to feed the upstream channel and the other branch to balance the forcing and water level. As a result, tides convey more water in this branch resulting in the larger U_{M2}. For the simulation where the tides are equally imposed in the two branches, the U_{M2} in both branches are low with the equal magnitude. Since the tides from both branches already have equal forcing, they do not balance each other. Therefore, the low U_{M2} is actually the character of the tide itself.

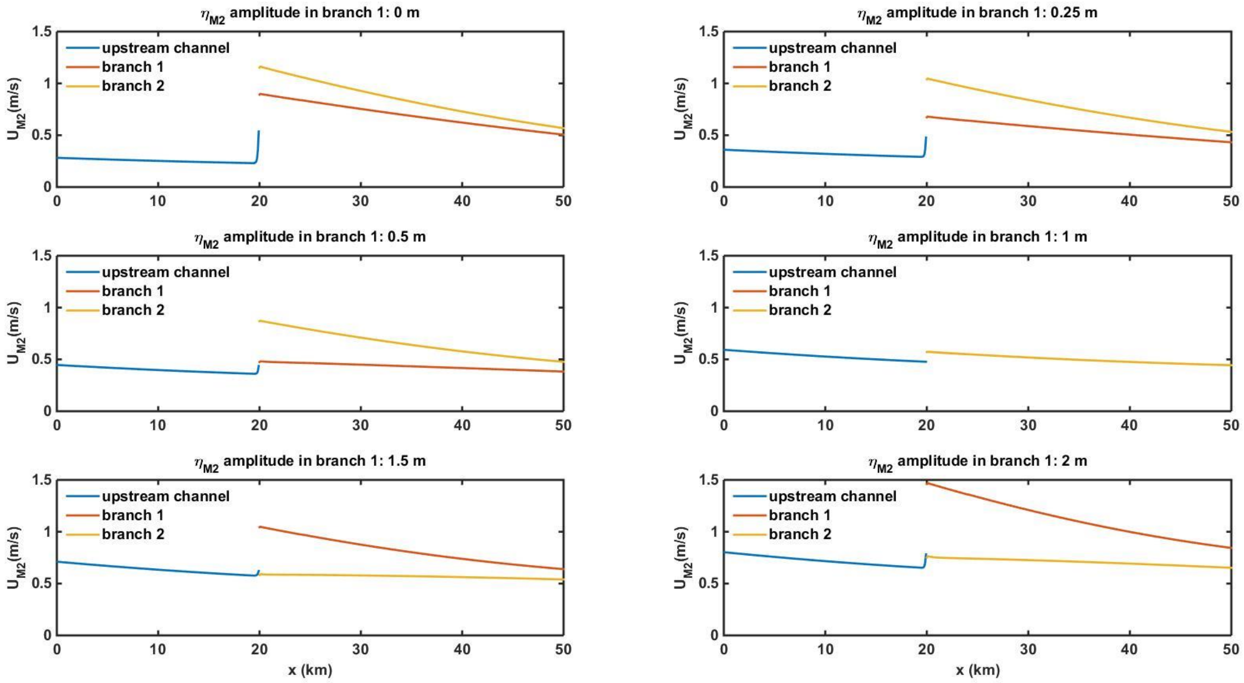

Figure 3-17. Each panel represents a width-averaged M2 velocity amplitude (U_{M2}) profile along the channel for different M_2 elevation amplitude imposed from the entrance of the branch 1 while M_2 elevation amplitude in branch 2 is 1 meter for all cases. Km 0 at the most left of each panel is the most upstream of the upstream channel at which the channel start diverging seaward.

The unequal tidal current and mean flow between branches cause the unequal sediment transport. The branch with larger tide shows a larger sediment transport except for the situation in which no tide is imposed from a branch. However, unequal tides condition causes an increasing of the sediment transport capacity in both branches. Figure 3-19 shows the tidally-averaged suspended sediment flux profile along the channel. It can be seen that though the sediment transport in unequal tidal forcing condition results in unequal sediment transport, the sediment transport in both branches for such a situation is much larger than for the equal tidal forcing condition. A larger transport capacity is mainly because one branch conveys a large U_{M2} while the other branch has a large mean flow. The same pattern also occurs in the bedload spatial profile that can be seen in Figure 3-20.

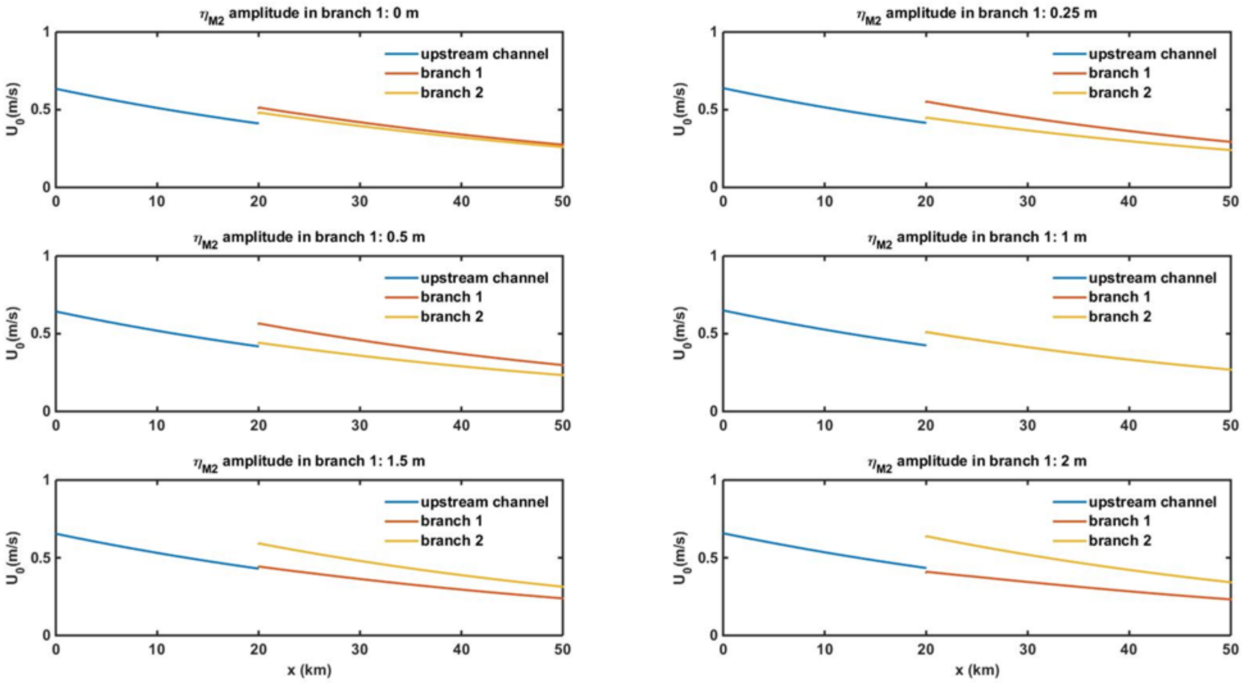

Figure 3-18. Each panel represents a width-averaged mean flow (U_0) profile along the channel for different M_2 elevation amplitude imposed from the entrance of the branch 1 while M_2 elevation amplitude in branch 2 is 1 meter for all cases. Km 0 at the most left of each panel is the most upstream of the upstream channel at which the channel start diverging seaward.

From the suspended sediment flux profile, it can be seen the increasing quantity nearby the junction toward the sea in both branches indicating the erosion occurs in both branches if the advection term is important. However if we compare to the long-term simulation (Figure 3-15), the advection seems to be relevant for the initial morphological evolution at which the erosion only occur nearby the junction. Then the sediment transport non-linearity causes the erosion to expand downstream.

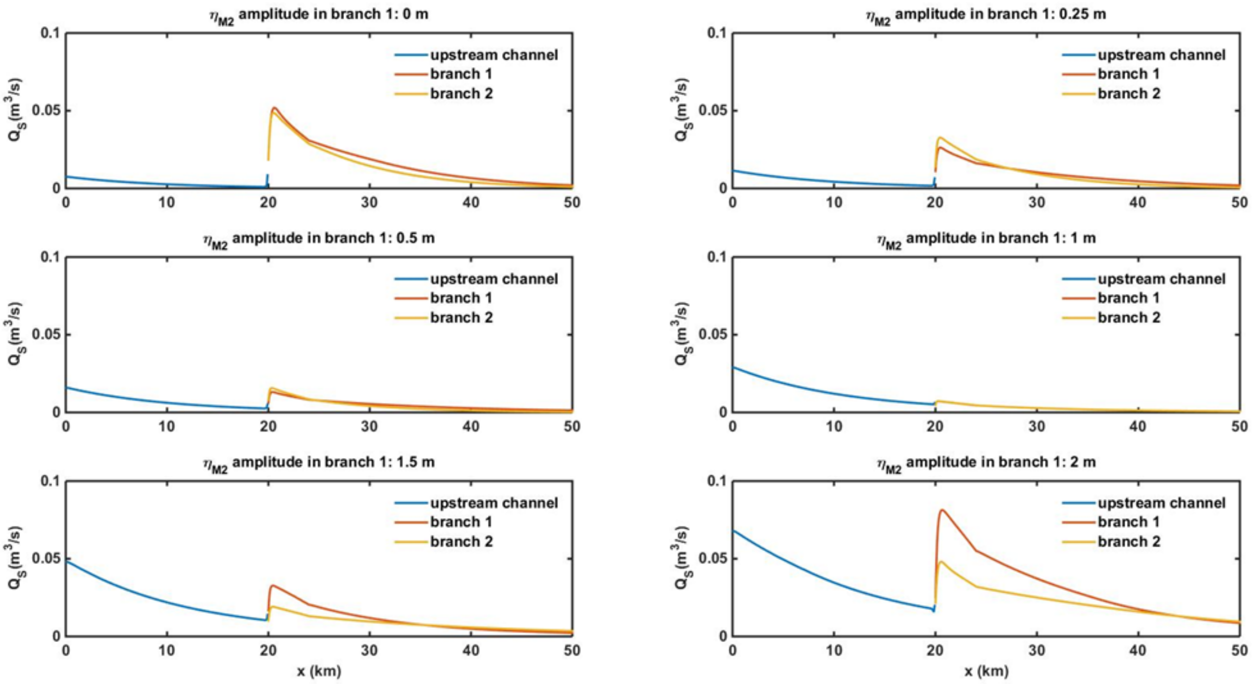

Figure 3-19. Each panel represents tidally-averaged suspended load flux (Q_S) profile along the channel for different M2 elevation amplitude imposed from the entrance of the branch 1, while M2 elevation amplitude in branch 2 is 1 meter for all cases. Km 0 at the most left of each panel is the most upstream of the upstream channel at which the channel start diverging seaward.

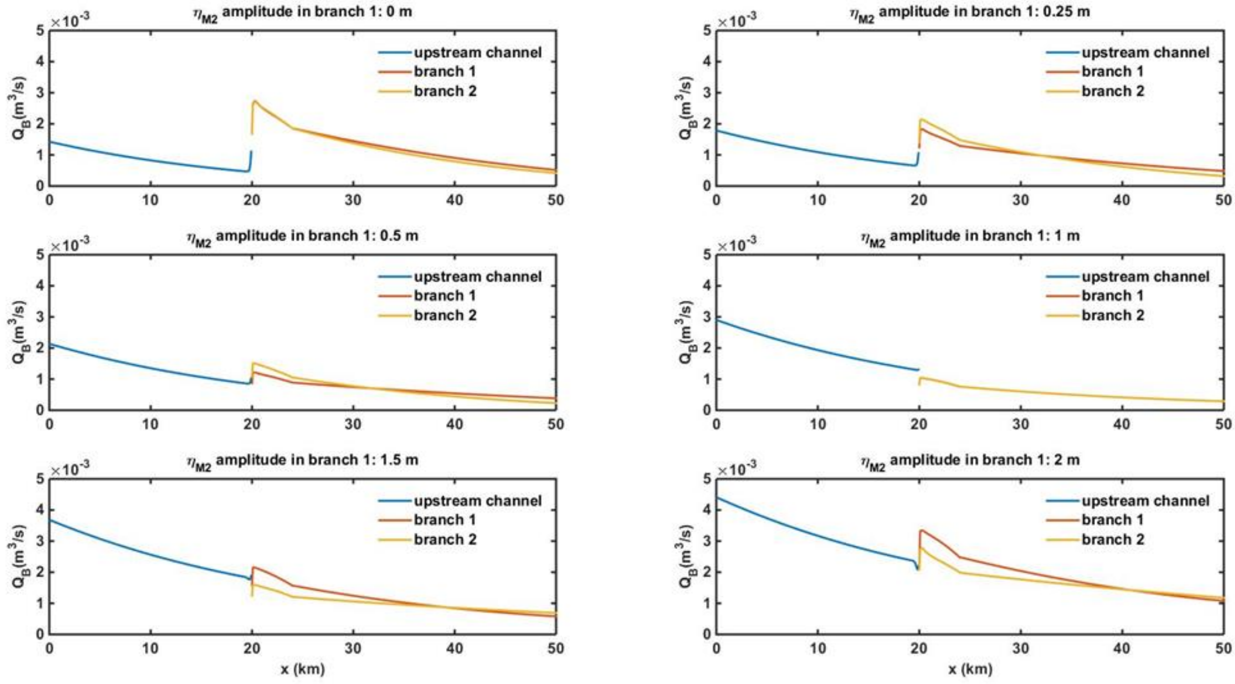

Figure 3-20. Each panel represents width integrated, depth-averaged and tidally-averaged bedload (Q_B) profile along the channel for different M2 elevation amplitude imposed from the entrance of the branch 1. Km 0 at the most left of each panel is the most upstream of the upstream channel at which the channel start diverging seaward.

3.2.2 Tidal Elevation Phase Difference Scenario

Figure 3-21 shows the morphological evolution nearby the junction for the case of 22.5 phase lag (small phase difference) and 45 degrees phase lag (larger phase difference). The lower tidal phase lagged causes the morphological instability of the junction where the silting up occurs in the branch with lagged tidal phase. When the tidal phase lagged is increased, the silting up of the branch with lagged tidal phase seems to be delayed (Figure 3-27). Then the larger tidal phase delay also results in the presence of subtidal trench at the junction. It indicates that the cross flow becomes larger (Figure 3-22) and, therefore, more important in determining the morphological evolution.

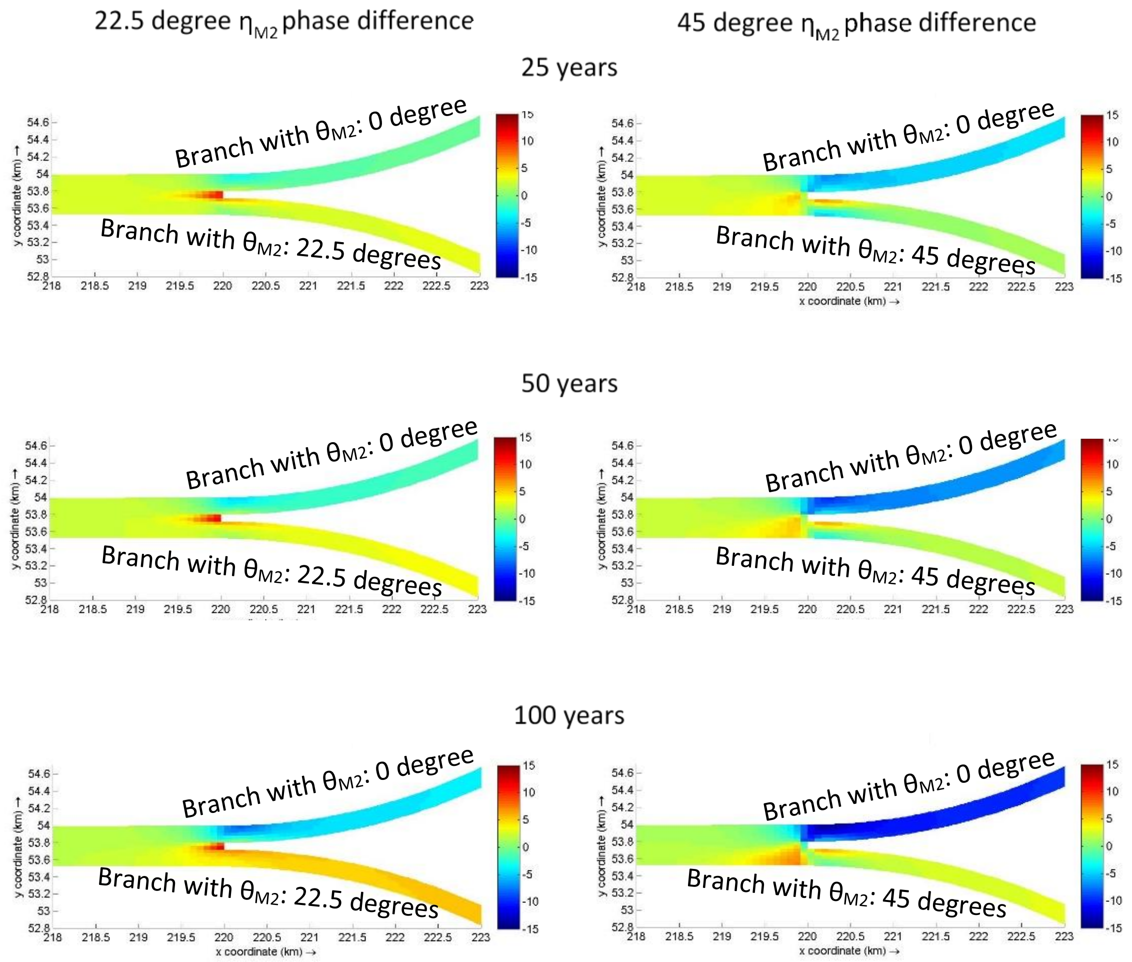

Figure 3-21. Erosion and deposition pattern for 100 years simulation at the junction. The left panels are the case of 22.5 degrees M2 elevation phase lag, and the right panels are the case of 45 degrees M2 elevation phase delay. The branch with earlier M2 phase (θ_{M2} = 0 degree) is the upper branch and the branch with lagged M2 phase ((θ_{M2} = 22.5 degrees (left panels) and 45 degrees (right panels)) is the bottom branch.

Figure 3-22 shows the M_2 tide cross-flow amplitude (V_{M2}) and the mean cross flow (V_0) for different tides situation over an M_2 period. The tidal phase difference between branches results in a partial tidal propagation from the branch with earlier tidal phase to another branch. The tide that comes earlier to the junction start feeding in the upstream channel and the other branch before the delayed tide comes. Then the propagation from one branch to another increases the cross-flow. More phase difference causes more water to be conveyed from one branch to another by the tide. Thus, the cross flow also increases with the increasing of the phase difference. Though the mean cross flow at the junction is small in all tidal phase situations, the M_2 cross-current increases with the increasing of the phase difference. The low mean flow and large V_{M2} indicates the cross flow is shifting in direction over an M_2 period. The increasing of V_{M2} with the larger phase difference results in the presence of subtidal trench in between the branches that occur in 45 degrees phase difference case in Figure 3-21.

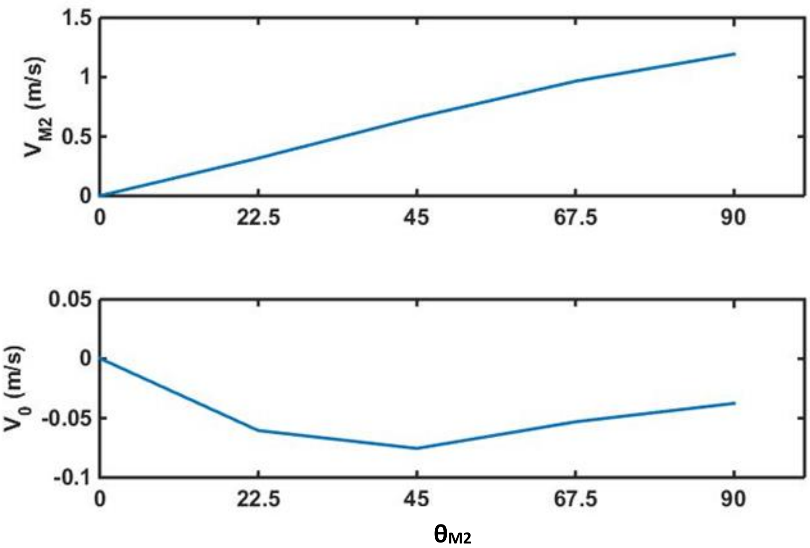

Figure 3-22. The M_2 tidal flow (top panel) and the mean flow (bottom panel) to the cross-channel direction in the middle of the upstream channel just before the junction for the different M_2 water elevation phase difference situations.

In along channel direction, the tidal propagation from one branch to another branch causes a lower mean flow (U_0) and larger M2 tidal current amplitude (U_{M2}) (Figure 3-23 and Figure 3-24) in the branch imposed by earlier tidal phase. Then the opposite behavior occurs in the branch with lagged tidal phase. The propagation from the branch with earlier tidal phase hampers the lagged phase tides that propagate in the other branch. Thus, it declines the tidal current and the tidal energy of lagged phase tides. The lower energy of lagged phase tide causes the river to be more conveying the branch with lagged tidal phase. As a result, the mean flow in the branch with lagged tidal phase is larger (Figure 3-23), and the U_{M2} is lower (Figure 3-24).

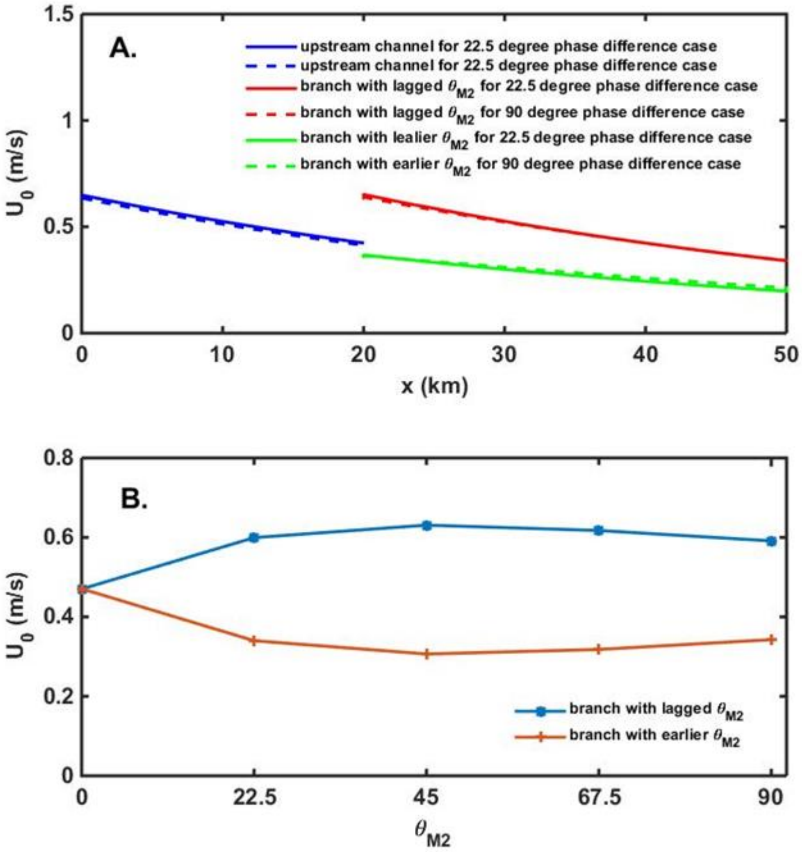

Figure 3-23. A) The width-averaged mean flow (U_0) profile along the channel for the cases of 22.5 (solid line) and 90 (dash line) degrees phase differences. Km 0 at the most left of the graph is the most upstream of the upstream channel at which the channel start diverging seaward. B) The mean flow at 4 km from the junction in both branches channel for all M2 elevation phase difference cases. The positive mean flow indicates the flow is to the seaward direction.

The small phase difference (22.5 degrees) results in a very low tidal current as shown in Figure 3-24. The U_{M2} in the branches with lagged tidal phase shows a decreasing profile landward instead of increasing as shown in the other branch. The increasing of phase lag causes the increasing of the U_{M2} in the branch with lagged tidal phase though the value is still smaller than the U_{M2} in the branch with earlier tidal phase. Then the U_{M2} shows the increasing pattern landward in both branches.

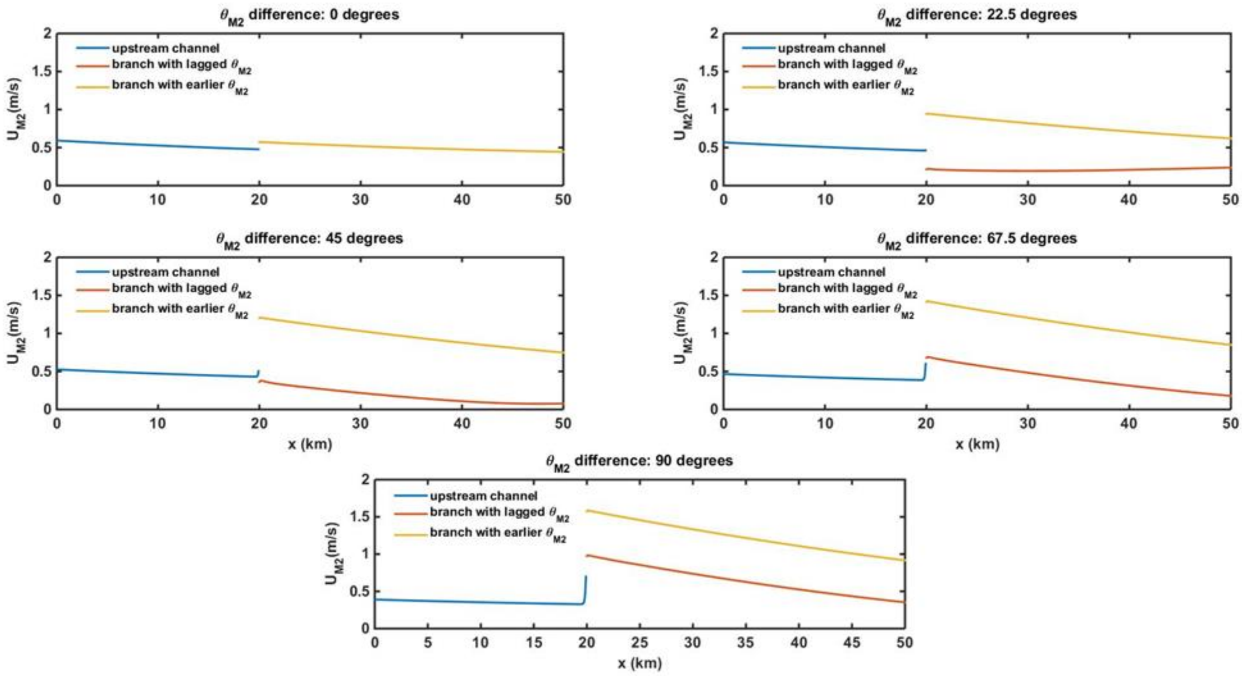

Figure 3-24. Each panel represents a width-averaged M2 velocity amplitude (U_{M2}) profile along the channel for different M2 elevation phase difference situations. Km 0 at the most left of each panel is the most upstream of the upstream channel at which the channel start diverging seaward.

In the branch with lagged tidal phase, the low U_{M2} for a small phase difference causes a very low transport capacity in the branch. While for a large tidal phase lagged, the increasing U_{M2} from to sea to the junction also increase a sediment transport capacity. Then the larger mean flow in this branch causes the sediment transport capacity to be more similar to the capacity in the branch with earlier tidal phase. This processes can be seen from tidally-averaged suspended load flux (Q_S) spatial profile in Figure 3-25. Compared to the case without phase difference, the phase difference causes sediment transport to be larger in both branches except for the case with a phase lag of 22.5 degrees. It indicates the more sediment transport capacity in both branches with the large phase difference. The similar behavior is only obtained for the tidally-averaged bedload flux in Figure 3-26.

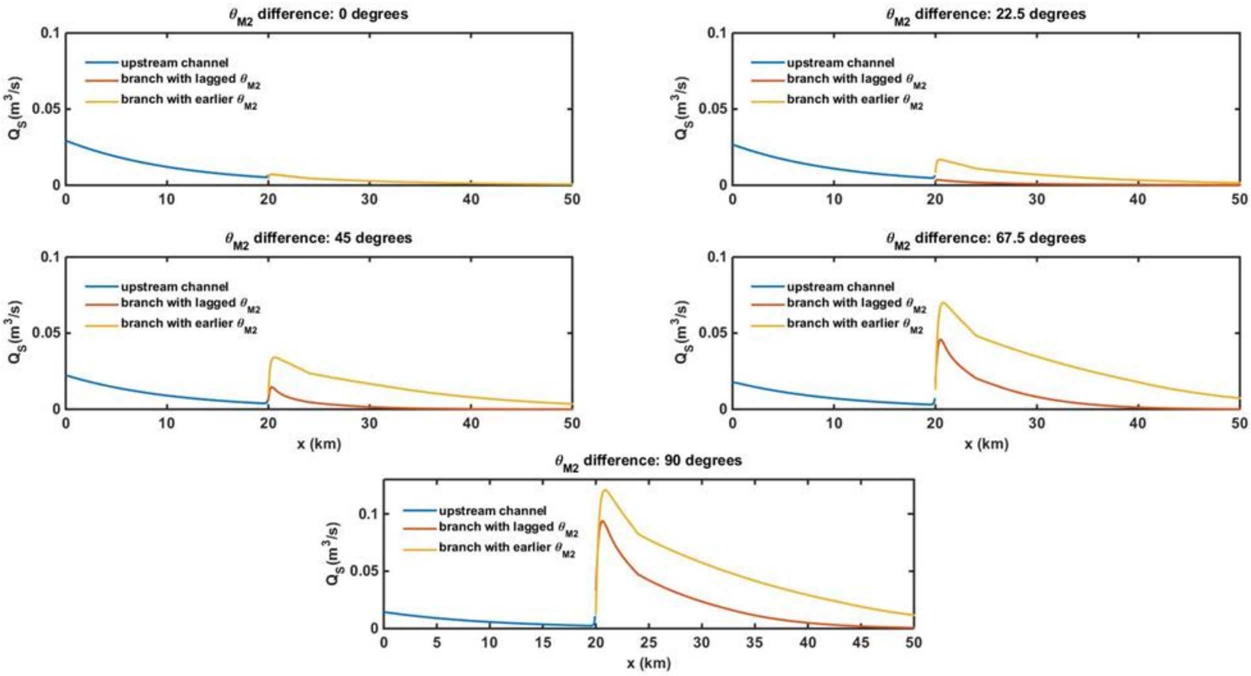

Figure 3-25. Each panel represents a width integrated, depth-averaged and tidally-averaged suspended load (Q_S) profile along the channel for different M2 elevation phase difference situations. Km 0 at the most left of each panel is the most upstream of the upstream channel at which the channel start diverging seaward.

The increasing Q_S nearby the junction indicates the erosion in both branches if the advection effect is significant. However, from the long-term simulation (Figure 3-21), the morphological evolution seems to be more influenced by the bar development and the sediment transport non-linearity enhances it. Figure 3-27 shows the bed erosion/deposition time series in the branch with lagged tidal phase just after the junction. It can be seen that, in the initial morphological development, the advection influences the process. It is indicated by the erosion at this location before 20 years which is at the same location where the sediment transport increases in the short-term simulation. However, after 20 years, the migrating bar from the upstream takes over the morphological development of the junction. The deposition occurs at this location due to the weaker current while the other branch is eroded. The sediment transport non-linearity increases the inequality of the morphological development of both branches.

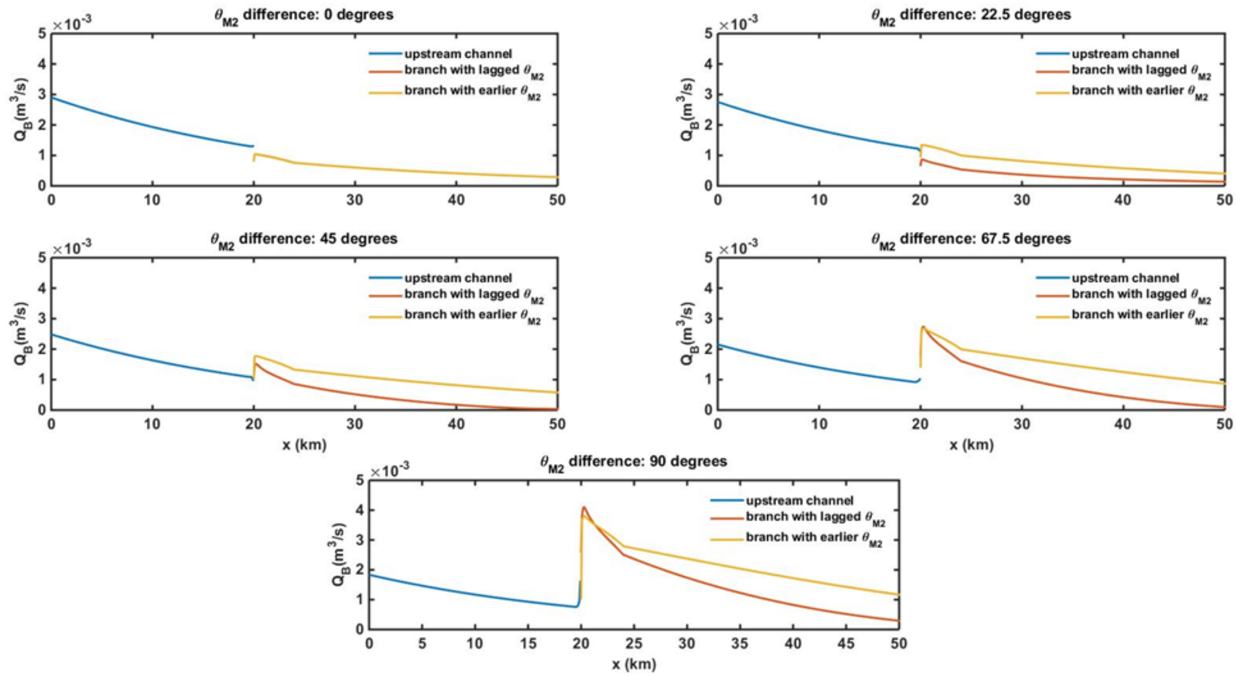

Figure 3-26. Each panel represents tidally-averaged bedload flux (Q_B) profile along the channel for different M2 elevation phase difference situation. Km 0 at the most left of each panel is the most upstream of the upstream channel at which the channel start diverging seaward.

For the small phase difference between branches, a weak cross-channel current at the junction is not sufficient to erode the fixed bar in the middle of the upstream channel at the junction (Figure 3-21). Then the migrating bar enhances the fix bar growth and causes the silting up in the branch with lagged tidal phase. The silting up in this branch is due to the weak U_{M2} that is not sufficient to erode the bed. The silting up is constant in a hundred year simulation (Figure 3-27). Therefore, the small phase difference causes the morphological instability of the junction whereby the branch with lagged tidal phase will be closed off.

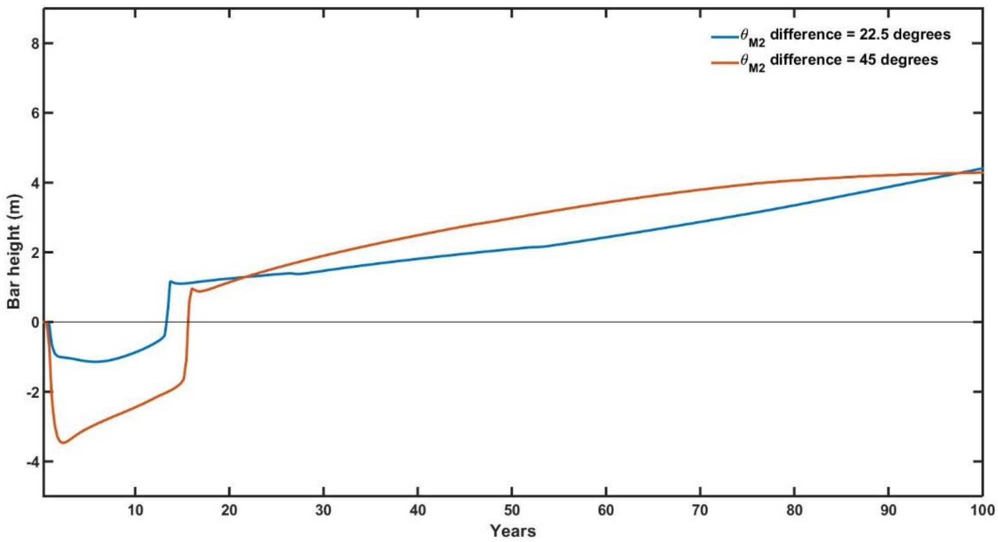

Figure 3-27. The bed evolution over a hundred-year simulation for two different M_2 phase difference cases.

When the tidal phase difference is increased, more water is conveyed from one branch to the other by the tide. It causes a larger cross-channel flow at the junction. The larger cross flow seems to be sufficient to keep both branches open in the longer time. This situation occurs because a larger cross flow could erode the bed at the junction which can be indicated by the presence of trench to connect the branches at the junction. The sediment brought from that erosion cannot be fully transported in the branch with lagged tidal phase. The bar on the inner side of the branch and in the upstream channel on the side of the regarding branch develops due to the horizontal turbulent of the cross-channel flow. Since the U_{M2} in the branch is low, the along channel current in the branch is insufficient to erode the bars. In a hundred years of simulation, the bars seem to grow in height, but the growth is slowing down in a hundred years (Figure 3-27).

It can be concluded that though phase difference causes the asymmetrical sediment discharge and river flow, larger phase difference could keep both branches to open for a longer period. Even in the largest phase difference case (90 degrees), the current can erodes the bed of both branches at the junction that causes more both branches to keep open almost symmetrically.

3.3 The Influences of Tides to the Morphological evolution

From all simulations, it can be summarized that the morphological evolution of the junction is controlled by two factors. *First*, the bar development and the junction morphological instability strongly depend on the inequality of the along channel tidal current (U_{M2}) and the mean flow (U_0) in along between branches. The U_{M2} is controlling the sediment entrainment from the bed while the U_0 is transporting the sediment. The larger U_{M2} and U_0 in one branch cause the erosion in the branch and silting up in the other branch. In the case of U_{M2} is dominant in one branch and U_0 in the other one, both currents seem to compete to keep the branch open. For instance, in the tidal phase difference situation between branches, the 22.5 degrees phase difference causes the close off in the branch with Larger U_0 and lower U_{M2}. However, in the amplitude difference scenario, the branch with the similar behavior experiences erosion. The latter is happening due to the tidal propagation from one branch to another to balance the water level and, in turn, the tidal energy. This process causes the significant magnitude of cross flow at the junction. Therefore, the *second* factor that controls the morphological evolution of the junction is the cross flow. The erosion at the junction seems to occur when M_2 tide cross flow amplitude (V_{M2}) is large and not necessary for the V_0. The large V_{M2} erodes the bar and cancels its development. The erosion forms a trench connecting the branches. Then the sediment from the trench is transported by the along channel current to the sea.

In the most case of the real estuaries, the branches of the bifurcation have a different geometry such as different depth or length. This condition could lead to avulsion, yet, in most cases, the junction seems to be stable where both branches are open. The unequal tidal forcing with counteracting effect in morphological evolution is required in such junctions to stabilize the junction in which both branches keep open. Therefore, two simulations is run to investigate it. The first simulation, the depth difference branches situation is combined with the amplitude difference scenario. The deeper channel that experience erosion is imposed by the large M_2 tide (M_2 amplitude = 1 meter) and the shallower branch is imposed by the lower M_2 tide (M_2 amplitude = 0.25 meter). The second simulation is that the depth difference branches situation is combined with the amplitude difference scenario. The deeper channel that experience erosion is imposed by the lagged M_2 water level phase (M_2 phase = 45 degrees). Whereas the shallower branch is imposed by the earlier M_2 tidal phase (M_2 phase = 0 degree).

It can be seen in the left panels of Figure 3-28, the amplitude difference between branches can balance the effect of depth difference to the morphological evolution. Though the bar in the upstream channel on the side of shallower branch still exists, its size shrinks in a hundred years. The cross channel current due to the tidal propagation from shallower branch to the deeper branch results in a trench-like erosion in between the branches. Top panel of Figure 3-29 shows the bed evolution time series in a hundred years in the middle of the branches just after the junction. It can be seen that in the shallower branch, the competition between the amplitude difference effect and the bar development due to depth difference results in an almost stable bed. The significant deposition after 50 years is because the presence of the migration bar from the upstream at that location. The effect of the migration bar also causes a bit siltation in the deeper branch. However, after this siltation both branch experience erosion until 100 years.

The 45 degrees phase difference gives the opposite result with the depth difference scenario. The deeper branch seems to silt up while erosion takes place in the shallower branch. It can be seen in the right panels of Figure 3-28, in the first 25 years, the effect of depth difference appears where the fixed bar grows in the middle of the upstream channel and widens to the shallower branch side. On the other hand, deeper branch experiences erosion. However, after a hundred years, the effect of phase difference takes over the effect of depth difference. The bar development occurs on the side of deeper branch which has a lagged tidal phase while the erosion takes place on the side of shallower branch. This morphological evolution pattern becomes more similar with the phase difference scenario with 45 degrees tidal phase lagged and symmetrical junction which can be seen in Figure 3-21. The bottom panel of Figure 3-29 shows the time series of the bed change in the middle of the branches just after the junction. The initial bed change in shallower branch shows a small deposition that might be due to the depth difference effect. However, it is followed by the erosion trend. After 20 years, the migration bar causes a significant accretion. However, the bed is eroded continuously until a hundred years. The initial bed change of the deeper branch in this simulation is also similar with the depth difference scenario where the large erosion takes place in this branch. The lagged tidal phase effect in this branch causes a deposition trend after the migration bar pass through the junction after about 20 years. However, the deposition trend is slowing down and showing a small erosion pattern several years before a hundred years. The phase difference effect causes a cross flow that is sufficient to erode bar development at the junction occurring the trench in between the branch. With that being said, the phase lagged between branches can counteract the junction instability due to the depth difference. The earlier tides should come from the branch that tends to close off. In the real estuaries, this condition can be reached by the different condition the downstream of both branches. For instance, the deeper branch is connected to the more complex channel networks and much longer distance to the sea than the shallower branch.

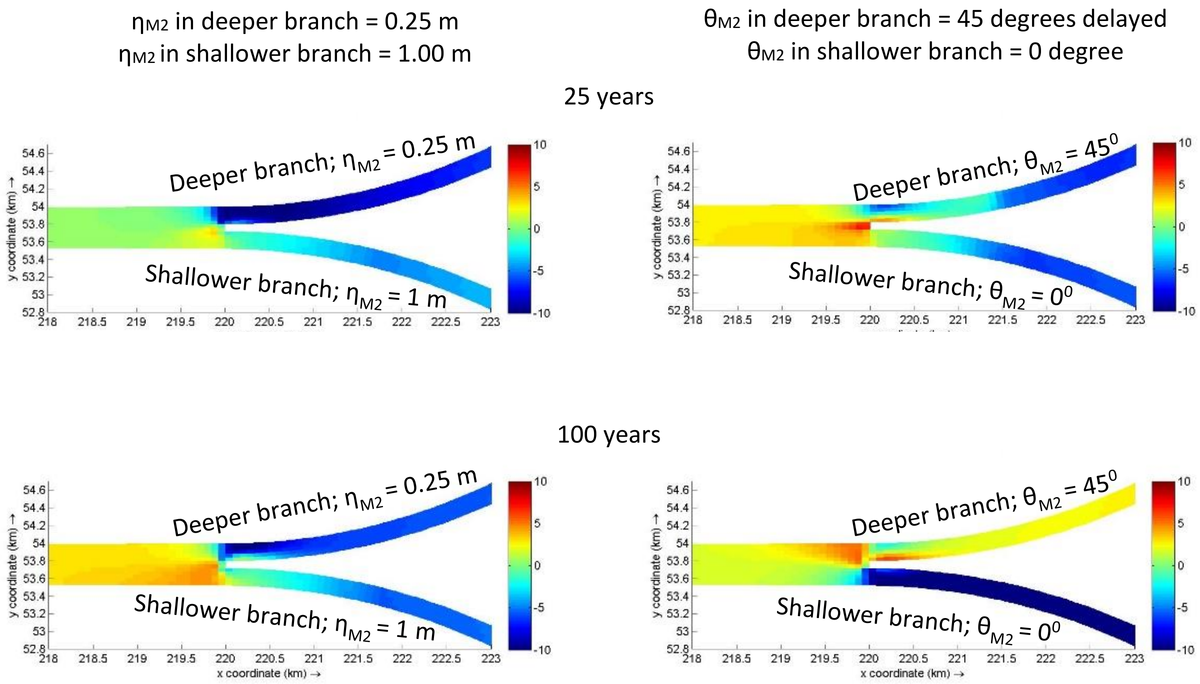

Figure 3-28. Erosion and deposition pattern for 100 years simulation at the junction. The left panels are the case of the depth difference opposed by the amplitude difference, and the depth difference opposed by the tidal phase difference. The branch with earlier M_2 phase (θ_{M2} = 0 degree) is the upper branch and the branch with lagged M_2 phase ((θ_{M2} = 22.5 degrees (left panels) and 45 degrees (right panels)) is the bottom branch.

The unequal tidal forcing can have two roles in stabilizing the morphologically unstable junction. First, it can erode the river bed at the junction canceling the bar formation and resulting in the trench between the branches and erosion in both branches. Secondly, the tidal forcing difference balances the effect of geometry difference by causing the opposites effect to the morphological development of the junction as present for the simulation of phase difference opposed by depth difference.

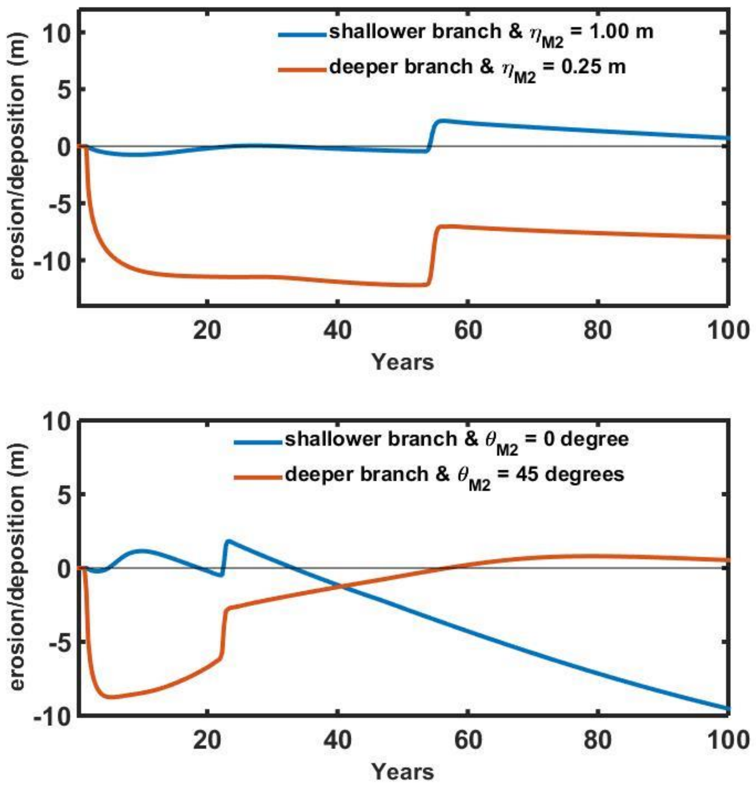

Figure 3-29. Top panel: the erosion/deposition time series in the middle of the branches just after the junction for the amplitude difference opposed by the depth difference. Bottom panel: the erosion/deposition time series in the middle of the branches just after the junction for the tidal difference opposed by the depth difference.

4 Discussion

4.1 The Effect of Tides to the Morphological Stability of the Junction

From this study, it reveals that the along-channel tidal flow inequality in the branches and the cross flow at the junction determine the morphological stability of the junction, whether both branches are open, or one branch is closed. Therefore, the influence of the tide to the morphodynamics of tidal junction can be illustrated by Figure 4-1.

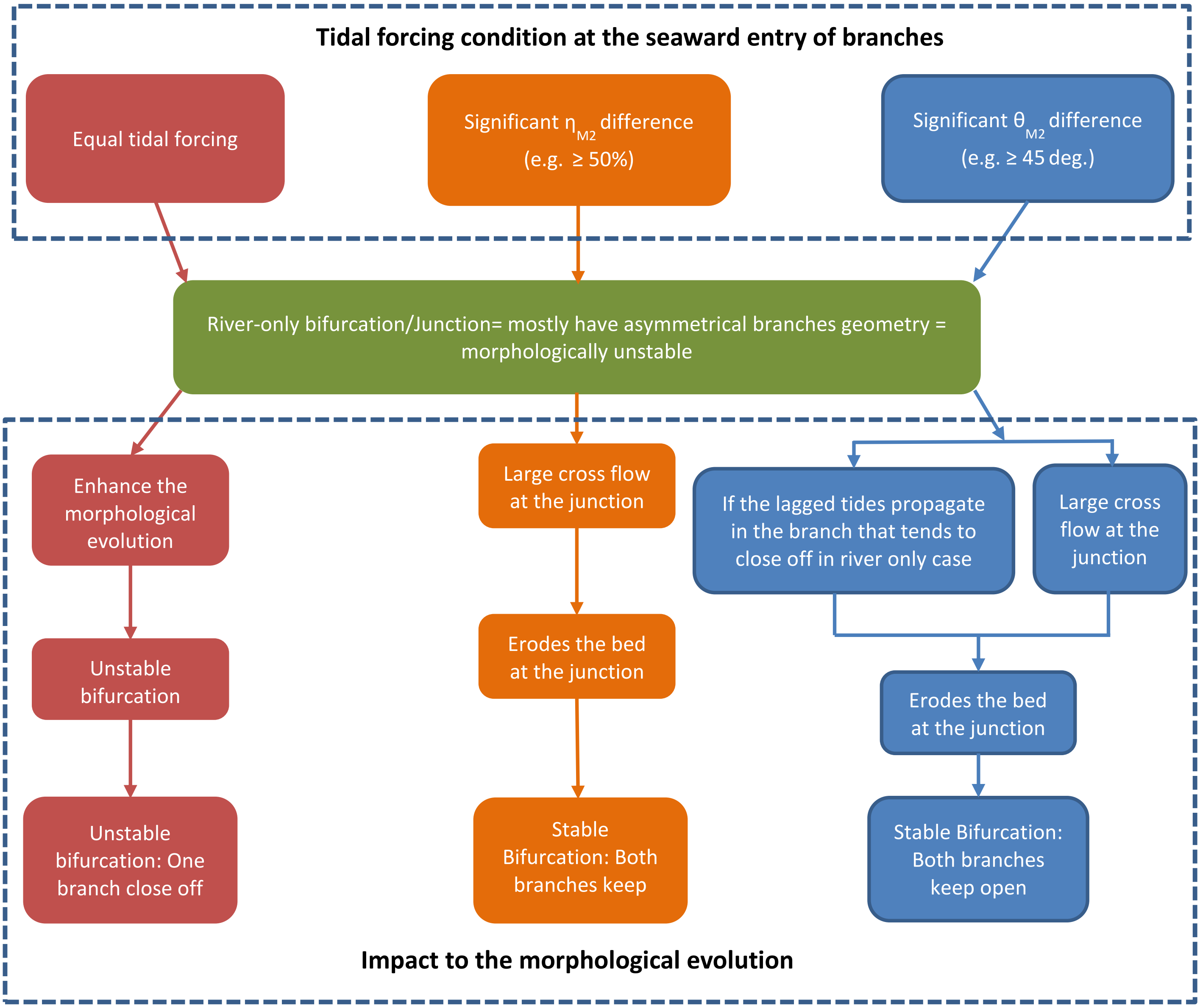

Figure 4-1. The illustration of the effect of the tides to the junction morphological evolution for several tidal forcing situation.

The equal tidal forcing at the seaward entry of the branches can enhance the morphological evolution that would occur in a river-only situation as investigated by *Pittaluga et al. (2003)* and *Kleinhans et al. (2008).* The tidal current seems to behave in the same way as the river discharge where tidal current is larger in the branch with the dominant river discharge in the river-only situation. Thus, the erosion is enhanced in this branch with the presence of tide. While in the branch with lower river discharge, the tidal current is also lower. As a result, the presence of tide also increases the inequality of water discharge division as modeled by *(Buschman et al., 2011)*.

On the other hand, a significant tidal forcing inequality can counteract the junction morphological instability that would occur in the river bifurcation. In this study, the unequal tidal forcing is made at the sea. However, in the real estuaries, the tidal phase or amplitude coming to the bifurcation from the branches could be different due to the branches geometry *(Buschman et al., 2013; Sassi et al., 2011 & 2013)* or the downstream condition. Regarding the downstream condition of the branches, both branches could have different downstream conditions such as a complexity of the channel networks on the downstream, distance to the sea, or anthropogenic interference.

The tidal forcing inequality could cause tidal propagation from one branch to another. Then it induces the large cross flow at the junction that erodes the bed at the junction. The erosion is illustrated by the appearance of the trench between the branches in Figure 3-15, and left panels of Figure 3-28 for tidal amplitude difference case. The presence of the trench due to the cross flow in different tidal forcing condition also can be seen in phase difference scenario for the cases of phase difference more than 22.5 degrees (Figure 3-21). The periodical erosion, therefore, causes the trench and the bathymetry at the junction to be deeper and consequently keep both branches open as observed by *Buschman et al. (2013)* in Berau Estuaries.

The role of cross flow and the bar development in the upstream channel are important to determine the junction morphological stability. Therefore, the two-dimensional the 1D concept by *Wang et al. (1995)* without the two-dimensional effect *(Wang & Ding, 2012)* is not suitable to investigate the morphological evolution of the junction. The 2D parameterization will be required to take into account if the morphological development model is applied to the 1D model. Further, the 1D model should accommodate the settling and scour lag effects in the gradually varied flow condition *(Sassi et al., 2013)* due to the tides that did not take into account in the *Pittaluga et al. (2003)* and *Kleinhans et al. (2008)*.

4.2 Future Research

The morphological evolution is a long-term process that can take hundreds or thousands of years until it reaches its equilibrium condition. 3D and 2D model is computationally expensive for such a long-term period so that the 1D model will be more suitable. Therefore, the 1D model (Wang et al, 1995) with 2D effect used *Pittaluga et al. (2003), Kleinhans et al. (2008, 2011)* need to be extended by tides. The 1D model can also be very useful to model an evolution of the entire delta with many channel networks and tidal creek system.

From this study, it is revealed that the geometry difference effect to morphological development can be opposed by the unequal tidal forcing. However, the sensitivity of the stability to the geometry difference in unequal tides condition also needs to have further studies. Geometry differences that occur in the estuary are also variable, such as, the branches are different in slope, width, meandering upstream channel shape or e-folding length scale. Those geometry differences might have a different degree of tidal inequality between branches.

The river discharge condition is also important to the morphodynamics of the junction. In this study, the river discharge forcing is relatively strong to maintain overdamped bar regime condition in the river-only situation. The weak river discharge condition might give a different result since the tidal energy would be less hampered. Then it also influences the bar regime *(Kleinhans and van den Berg, 2010)*. The tidal junction morphological evolution in the underdamped bar regime condition might be different to the overdamped condition.

The presence of the intertidal might affect the tides since the considerable tidal flat area compared to the channel area can change the dominant tidal flow direction (Friedrichs, 2012). The tidal flow direction in this term is the flood and ebb direction. The change in the dominant direction might also change the tidally-averaged sediment transport as well as the morphological development.

The salt intrusion seems to have an important role in transporting the sediment *(van Kessel et al., 2011).* The effect of salt intrusion process in the tidal junction examined by *de Swart (2015)* might give a significant effect to the morphological evolution of the junctions.

5 Conclusions

This chapter presents the conclusion of the effect of tides in morphological evolution of the tidally-influenced junction using idealized junction model. It can be concluded that:

- For the equal tide with unequal geometry, the equal tidal forcing enhances sediment transport capacity that might occur in river only situation. More sediment erodes from the bed at the erosion location and settles at deposition location that would occur in the river only situation. Therefore, the morphological evolution of the junction that occurs in the river only situation is enhanced by the tide. It can be said that the tides enhance morphological instability of the bifurcation in this case.
- Tidal elevation amplitude difference between branches increases the sediment transport capacity in both branches and induces the current from one branch to another. The implication to the morphology is that the current from one branch to another causes the erosion at the junction and the large transport capacity in both branches cause the deepening of the two branches. As a result, the bifurcation is morphologically stable.
- Small tidal phase difference results in a weak sediment transport capacity in the branch with lagged tidal phase. This condition causes the morphological instability where the branch with lagged tidal phase silts up and tends to close while the other deepens. By increasing the phase difference the closure of one branch is delayed.

Therefore, The Tidally-influenced junction will be stable if either the tidal amplitude or the tidal phase in both branches is significantly unequal. For the cases that the branches geometry is unequal, the tidal forcing inequality with the opposing effect to the unequal geometry is required to keep the two branches of the junction open.

Acknowledgment

Thank you to Maarten van der Vegt and Maarten Kleinhans for your support, knowledge, and motivation in writing this thesis, Tyas for always throwing me a buoy when I was drowning in the splitting channel, my parents for giving me inspiration. Lembaga Pengelola Dana Pendidikan (LPDP) scholarship for giving me the opportunity to study abroad. Last but not least, all praise belongs to Allah.

Referencess

Bagnold, R., 1966. An Approach to the Sediment Transport Problem From General Physics. Washington: US Government Printing Office.

Bolla Pittaluga, M., Repetto, R., & Tubino, M. (2003). Channel bifurcation in braided rivers: Equilibrium configurations and stability. Water Resources Research, 39(3), 1–13. http://doi.org/10.1029/2003WR002754

Buschman, F. A., Hoitink, A. J. F., van der Vegt, M., & Hoekstra, P. (2010). Subtidal flow division at a shallow tidal junction. Water Resources Research, 46(12), W12515. http://doi.org/10.1029/2010WR009266

Buschman, F. a., van der Vegt, M., Hoitink, a. J. F., & Hoekstra, P. (2013). Water and suspended sediment division at a stratified tidal junction. Journal of Geophysical Research: Oceans, 118(3), 1459–1472. http://doi.org/10.1002/jgrc.20124

Crosato, A. & Mosselman, E., 2009. Simple physics-based predictor for the number of river bars and the transition between meandering and braiding. Water Resources Research, Volume 45, p. W03424.

Dissanayake, D. M. P. K., Ranasinghe, R., & Roelvink, J. a. (2009). Effect of Sea Level Rise in Tidal Inlet Evolution: A Numerical Modelling Approach. Journal of Coastal Research, 2009(56), 942–946. Retrieved from <Go to ISI>://WOS:000266722400007

Dissanayake, D. M. P. K., Roelvink, J. a., & van der Wegen, M. (2009). Modelled channel patterns in a schematized tidal inlet. Coastal Engineering, 56(11-12), 1069–1083. http://doi.org/10.1016/j.coastaleng.2009.08.008

de Swart, R., 2015. A modelling study on salinity intrusion and tidal propagation in estuarine channel networks with different channel lengths using the Delft3D software package (Msc Thesis), Utrecht: Utrecht University.

Hill, a. E., & Souza, a. J. (2006). Tidal dynamics in channels: 2. Complex channel networks. Journal of Geophysical Research: Oceans, 111(April), 1–9. http://doi.org/10.1029/2006JC003670

Ikeda, S., 1982. Incipient Motion of Sand Particles on Side Slopes. Journal of Hydraulics Division, ASCE, 108(1), pp. 95-114.

Jones, O. P., Petersen, O. & Kofoed-Hansen, H., 2007. Modelling of complex coastal environments: Some considerations for best practice. Coastal Engineering, Volume 54, pp. 717-733.

Kleinhans, M. G., Jagers, H. R. a, Mosselman, E., & Sloff, C. J. (2008). Bifurcation dynamics and avulsion duration in meandering rivers by one-dimensional and three-dimensional models. Water Resources Research, 44(8), 1–31. http://doi.org/10.1029/2007WR005912

Kleinhans, M. G. & van den Berg, J. H., 2010. River channel and bar patterns explained and predicted by an empirical and a physics-based method. Earth Surface Processes and Landforms, Volume 36, pp. 721-738.

Kleinhans, M. G., de Haas, T., Lavooi, E. & Makaske, B., 2012. Evaluating competing hypotheses for the origin and dynamics of river anastomosis. Earth Surface Processes and Lanforms, Volume 37, pp. 1337-1351.

Kleinhans, M. G., Ferguson, R. I., Lane, S. N., & Hardy, R. J. (2013). Splitting rivers at their seams: Bifurcations and avulsion. Earth Surface Processes and Landforms, 38(1), 47–61. http://doi.org/10.1002/esp.3268

Koch, F. & Flokstra, C., 1981. Bed level computations for curved alluvial channels. In Proceedings of the XIX Congress of the International, Volume 2, p. 357.

Lesser, G., 2009. An approach to medium-term coastal morphological modeling, PhD-thesis. Delft: Delft University of Technology.

Mosselman, E., Turbino, M. & Zolezzi, G., 2006. The overdeepening theory in river morphodynamics: two decades of shifting interpretations. In River Flow 2006: International Conference on Fluvial Hydraulics, pp. 1175-1181.

Nugrahadi, M. S., 2005. Review studi estuari di Indonesia. alami, 10(3), pp. 18-22.

Parker, G., 1976. On the cause and characteristic scales of meandering and braiding in rivers. Journal of Fluid Mechanics, Volume 76, pp. 457-479.

Ranasinghe, R., Swinkels, C., Luijendijk, A., Roelvink, D., Bosboom, J., Stive, M., & Walstra, D. (2011). Morphodynamic upscaling with the MORFAC approach: Dependencies and sensitivities. Coastal Engineering, 58(8), 806–811. http://doi.org/10.1016/j.coastaleng.2011.03.010

Roelvink, J. a. (2006). Coastal morphodynamic evolution techniques. Coastal Engineering, 53(2-3), 277–287. http://doi.org/10.1016/j.coastaleng.2005.10.015

Sassi, M. G., Hoitink, a. J. F., De Brye, B., Vermeulen, B., & Deleersnijder, E. (2011). Tidal impact on the division of river discharge over distributary channels in the Mahakam Delta. Ocean Dynamics, 61(12), 2211–2228. http://doi.org/10.1007/s10236-011-0473-9

Sassi, M. G., Hoitink, A. J. F., Vermeulen, B., & Hidayat, H. (2013). Sediment discharge division at two tidally influenced river bifurcations. Water Resources Research, 49, 2119–2134. http://doi.org/10.1002/wrcr.20216

Stelling, G., 1984. On the construction of computational methods for shallow water flow problems. s.l.:Rijkswaterstaat.

Struiksma, N., Olesen, K. W., Flokstra, C., & De Vriend, H. J. (1985). Bed deformation in curved alluvial channels. Journal of Hydraulic Research, 23(1), 57–79. http://doi.org/10.1080/00221688509499377

Talmon, A., Struiksma, N. & Mierlo, M., 1995. Laboratory measurements of the direction of sediment transport on transverse alluvial-bed slopes. Journal of Hydraulic Research, Volume 33, pp. 495-517.

Tonnon, P., van Rijn, L. & Walstra, D., 2007. Morphodynamic modelling of tidal sand waves on the shoreface. Coastal Engineering, Volume 54, pp. 279-296.

van den Berg, J., 1995. Prediction of alluvial channel pattern of perennial rivers. Geomorphology, Volume 12, pp. 259-279.

van der Wegen, M., Wang, Z. B., Savenije, H. H. G. & Roelvink, J. A., 2008. Long-term morphodynamic evolution and energy dissipation in a coastal plain, tidal embayment. J. Geophysical. Research, Volume 113.

Van Der Wegen, M., & Roelvink, J. a. (2008). Long-term morphodynamic evolution of a tidal embayment using a two-dimensional, process-based model. Journal of Geophysical Research: Oceans, 113(3), 1–23. http://doi.org/10.1029/2006JC003983

van Kessel, T., Vanledde, J. & de Kok, J., 2011b. Continental Shelf Research. Development of a mud transport model for the Scheldt estuary, Volume 31, pp. S165-S181.

van Rijn, L. C., 1993. Principles of Sediment Transport in Rivers, Estuaries and Coastal Seas. Amsterdam: Aqua Publications.

van Rijn, L. C., 2001. General view on sand transport by currents and waves : data analysis and engineering modelling for uniform and graded sand (TRANSPOR 2000 and CROSMOR 2000 models), Delft, The Netherlands: Delft Hydraulics.

van Rijn, L. C., 2003. Sediment transport by currents and waves; general approximation formulae, Florida, USA: s.n.

Wang, Z. B., De Vries, M., Fokkink, R. J., & Langerak, a. (1995). Stability of river bifurcations in ID morphodynamic models. Journal of Hydraulic Research, 33(6), 739–750. http://doi.org/10.1080/00221689509498549

Wang, Z. & Ding, P., 2012. The Branching Channel Network in the Yangtze Estuary. Coastal Engineering.

Zhang, W. et al., 2014. Redistribution of the Suspended Sediment at the Apex Bifurcation in the Pearl River Network, South China. Journal of Coastal Research, 30(1), pp. 170-182.

Statement of originality of the Msc thesis

I declare that:

1. This is an original report, which is entirely my own work
2. Where I have made use of the ideas of the other writers, I have acknowledged the soure in all instances
3. Where I have used any diagram or visuals I have acknowledged the source in all instances
4. This report has not and will not be submitted elsewhere for academic assessment in any other academic course.

Student Data

Name: Arya Pamungkas Iwantoro

Registration Number: 4299744

Date March 9, 2016

Signature